DEPARTMENT OF THE INTERIOR
U.S. GEOLOGICAL SURVEY

An evaluation of the applicability of the telluric-electric and audio-magnetotelluric methods to mineral assessment on the Arabian Shield, Kingdom of Saudi Arabia

by

V. J. Flanigan[1/] and C. J. Zablocki

Open-File Report 84-425

Prepared for Ministry of Petroleum and Mineral Resources, Deputy Ministry for Mineral Resources, Jiddah, Kingdom of Saudi Arabia

This report is preliminary and has not been reviewed for conformity with U.S. Geological Survey editorial standards and stratigraphic nomenclature.

1/ U.S. Geological Survey
Denver, CO 80225

1984

CONTENTS

ILLUSTRATIONS

AN EVALUATION OF THE APPLICABILITY OF THE TELLURIC-ELECTRIC AND AUDIO-MAGNETOTELLURIC METHODS TO MINERAL ASSESSMENT ON THE ARABIAN SHIELD, KINGDOM OF SAUDI ARABIA

by

Vincent J. Flanigan[1]/ and Charles J. Zablocki

ABSTRACT

Feasibility studies of two electromagnetic methods were made in selected areas of the Jabal Hibshi (1:250,000) quadrangle, 26F, in the Kingdom of Saudi Arabia in March of 1983. The methods tested were the natural source-field telluric-electric and audio-magnetotelluric methods developed and extensively used in recent years by the U.S. Geological Survey in some of its domestic programs related to geothermal and mineral resource assessment. Results from limited studies in the Meshaheed district, the Jabal as Silsilah ring complex, and across a portion of the Raha fault zone clearly demonstrate the appropriateness of these sub-regional scale, reconnaissance-type studies to mineral resource assessment. The favorable results obtained are largely attributed to distinctive and large contrasts in the electrical resistivity of the major rock types encountered. It appears that the predominant controlling factor governing the rock resistivities is the amount of contained clay minerals. Accordingly, unaltered (specifically, non-argillic) igneous and metamorphic rocks have very high resistivities; metasedimentary rocks of the Murdama group that contain several percent clay minerals have intermediate values of resistivity; and highly altered rocks, containing abundant clay minerals, have very low values of resistivity. Water-filled fracture porosity may be a secondary, but important, factor in some settings. However, influences from variations in interstitial or intercrystalline, water-filled porosity are probably small because these types of porosity are generally low. It is reasonable to expect similar results in other areas within the Arabian Shield.

1/ U.S. Geological Survey, Denver, Colorado 80225

INTRODUCTION

Program documents related to the U.S. Geological Survey's mission of mineral resource appraisal clearly state the need for identifying new exploration targets. The adopted strategy for attaining such a goal in the best and most systematic manner has been to initially acquire the basic geologic, geochemical, and geophysical framework on a regional scale (1:100,000) followed by the compilation and synthesis of these data at a scale of 1:250,000. Potential targets identified through this process can then be studied with more detailed 1:25,000- to 1:5,000-scale investigations, and conceptual, ore-occurrence models can be developed, tested, and used in the search for economic mineral deposits. Under Program 5 (Geophysics and Geochemistry), both gravity and aeromagnetic data have been acquired and geologic models have been, and are being, developed from the analysis of these data at scales appropriate to the scope of the regional geologic mapping investigations. In the early part of 1402 AH, it was recognized that additional knowledge of the substructure within certain regions of interest might be gained through the application of sub-regional electromagnetic reconnaissance mapping techniques. Such techniques can provide important, cost-effective, and complementary sets of information useful in enhancing the knowledge of the structure and mineralogy of rocks at shallow to intermediate depths of several kilometers. Collectively, these electromagnetic techniques, used in conjunction with regional gravity and magnetic interpretations, can also provide a rational basis for deciding on the extent and types of costlier, but appropriate, follow-up detailed surveys. Specifically, it was felt that the most logical means for accomplishing such a task was to apply the natural source-field audio-magnetotelluric (AMT) and telluric-electric (TE) methods as they have been found to be exceptionally useful in similar-type domestic programs carried out by the U.S. Geological Survey (Hoover and others, 1976, 1981, 1982).

Accordingly, a project proposal was submitted and subsequently approved and established as subproject 5.04.01 within the work program of the Deputy Ministry for Mineral Resources for 1402/1403 AH. The primary objective of this subproject was to assess the applicability of these methods towards aiding in achieving the overall mineral resource assessment goals of the Mission. The findings from this evaluation would, in turn, form the basis for consideration of establishing these techniques as an integral part of the Saudi Arabian Mineral Resource Appraisal Program (SAMRAP). In the following, we address this objective by way of examples of the results obtained from studies carried out in several areas within the Jabal Hibshi (1:250,000) quadrangle, 26F, (fig. 1) in the Kingdom of Saudi Arabia in March of 1983. The rationale for selecting these areas was chiefly based on the

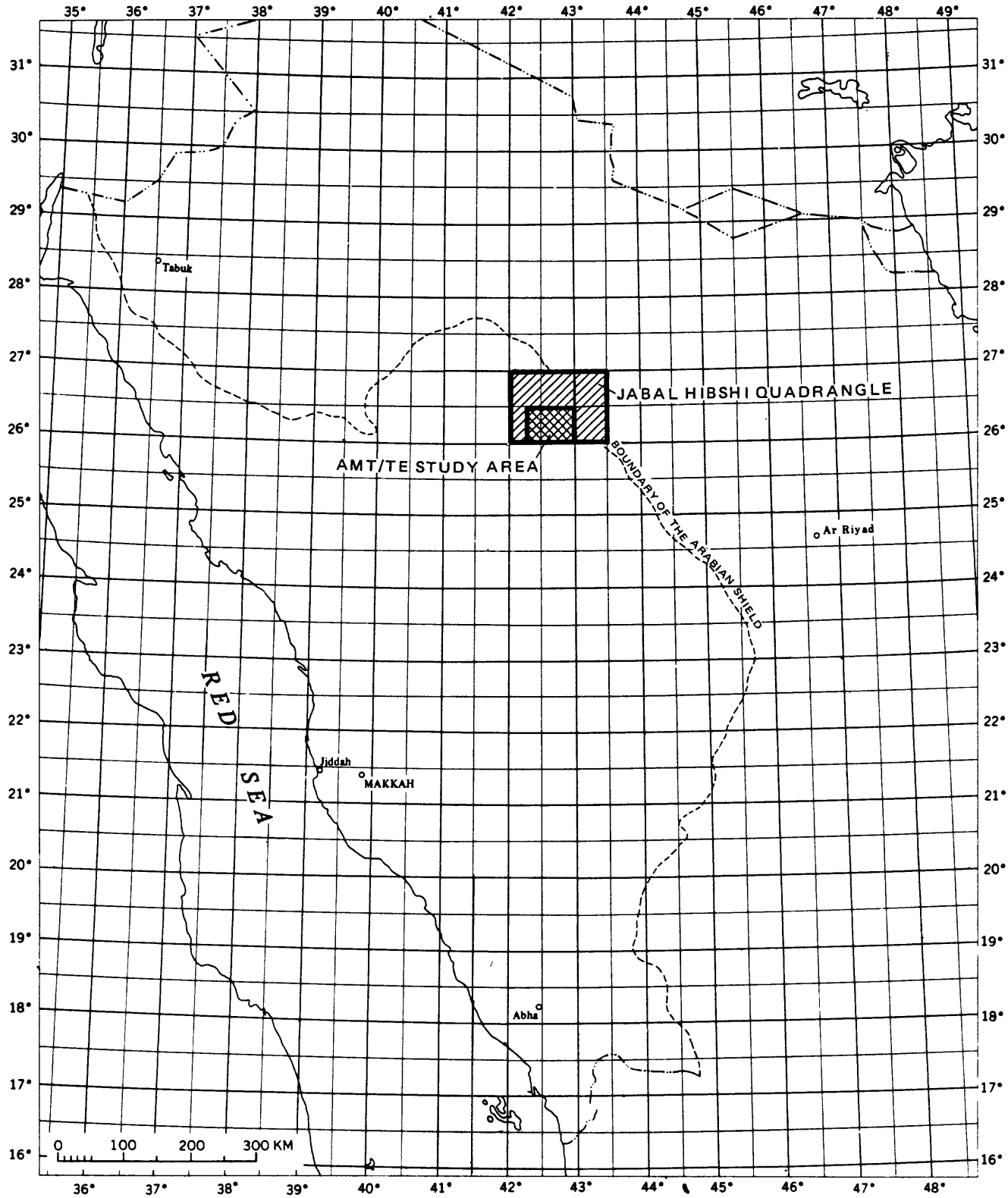

Figure 1.--Index map of western Saudi Arabia showing areas of Jabal Hibshi quadrangle, 26F, and electromagnetic studies.

fact that this quadrangle represents the USGS's initial area in which to demonstrate the appropriateness of the SAMRAP concept and in which there presently exist a fair amount of geologic, geochemical, and geophysical (aeromagnetic) information that could possibly provide some level of control in the interpretation of these results.

ACKNOWLEDGMENTS

The work on which this report is based was performed in accordance with an agreement between the Saudi Arabian Ministry of Petroleum and Mineral Resources and the U.S. Geological Survey (USGS). Information on the local geology of the Meshaheed area and of the Silsilah and Raha fault areas described in this report was provided by USGS geologists C. W. Smith and E. A. du Bray, respectively. These men also provided many constructive insights into the geologic implications of the results reported herein. To them, and the many others in the Mission who furnished the necessary logistical support for carrying out this study, we express our gratitude. Also, this report has benefited from technical review of an earlier version by C. L. Long (USGS, Denver, Colorado) who also developed the AMT data reduction and interpretive programs that were used in these studies.

THEORY AND TECHNIQUE

Electromagnetic field sources

Natural electromagnetic fields are generated virtually everywhere and continuously around the world. Low frequency (long period) time-varying changes below several hertz (Hz) generically result from sunspot activity. Solar winds (high energy plasma) interact with the earth's magnetosphere, which in turn, induces currents to flow in the ionosphere. These currents, in turn, create time-varying magnetic fields that couple with the finitely conductive earth to produce currents to flow within the earth. Thus, these latter currents are generally described as telluric currents.

Higher-frequency electromagnetic energy (from several Hz to about 10^4 Hz) results from world-wide lightning discharges in the lower atmosphere. The principal energy is derived from tropical storm cells that occur most frequently, but not exclusively, during the Northern Hemisphere summer months. These pulses, or spherics, propagate around the earth in the earth-ionosphere cavity (wave guide) to produce high-amplitude resonances, or so-called Schumann resonances, at about 8 Hz and certain multiples thereof. These electromagnetic fields are reflected and refracted at the earth's surface. Because of the resistivity contrast between the

atmosphere and the finitely conductive earth, the refracted component propogates vertically downward regardless of the incidence angle of the impinging wave. At large distances from the source, the relationship between the electric field and the orthogonal magnetic field component is everywhere constant for a uniformly conductive earth, i.e., the waves are considered to be planar. These higher-frequency waves (relative to the telluric-current type) are generally described as audio-magnetotelluric (AMT) waves.

Telluric-electric method

The telluric-electric (TE) method, or more exactly, the electric (E) field-ratio telluric profiling method, utilizes the aforementioned telluric currents as a source. The method basically consists of measuring the ratio of the resulting potential difference developed between two colinear grounded electrode pairs that share a common reference at the mid-point. That is, an array of three grounded electrodes are spaced equidistant and inline. If the azimuthal direction of the telluric currents is the same across each electrode pair, then the resulting potential difference for each pair will be proportional to the component of the telluric E field in the direction of the array. Further, if the section of ground between each electrode pair has the same electrical resistivity, then the resulting measured E-fields will be identical, or the ratio of these two fields will be unity. However, should the ground under one electrode pair contain higher or lower resistivity material than the other, the E-fields and their ratio will be different than unity. This can readily be seen from consideration of the point form of Ohm's Law ($E = jp$; where j is current density and p is resistivity). Thus, the objective of this method is to discern differences in the electrical resistivity of the rocks at shallow and/or deep depths (to several tens of kilometers) by measuring these ratios along a straight-line traverse. After the first ratio is measured, the three-electrode array is advanced forward one bipole length so that the forward electrode of the initial set-up becomes the center, or mid-point, reference electrode for the next ratio measurement. This "leapfrog" procedure is continued along the survey line to obtain a continuous set of relative electric-field intensity ratios. When successively multiplied together, these ratios yield a relative amplitude profile of the electric field along the traverse-line direction. This procedure is identically analogous to that of obtaining ground elevations using standard surveying techniques in which the base reference is "carried along" from each previous measurement. The analogy even extends to the practice of reversing the input leads from the two electrode pairs into the measuring system (similar to reversing the surveying rods) at each successive measurement location. In this way, errors resulting from any possible unequal voltage gains or offsets in the two channels of the

measuring system will not result in accumulating errors throughout the traverse.

The TE field ratio profiling system used in this study consisted of three non-polarizing electrodes, connected by a high tensile-strength insulated wire (250- or 500-m spacing) which was fed to an adjustable high-gain band-pass amplifier (20-second period high pass and 40-second period low pass). The band-pass setting was therefore set to largely measure telluric voltages centered about a 30-second period (about 0.033 Hz); a period which has been generally recognized as containing a consistently high-amplitude component in the telluric-field spectrum. After rectification and low-pass filtering, the output voltage from the two channels was fed into an X-Y graphic recorder. The resulting display on the chart produces a near-straight line from which the ratio of the two voltages can be determined by measuring the slope (i.e., tangent) of the line. Thus, for the situation in which the two electric field intensities are equal, the trace displayed on the X-Y plotter will be a straight line having a slope angle of 45 degrees. Similarly, if the voltages are unequal because of different resistivities in the vicinity of the electrode pairs, the slope will be different than 45 degrees. Figure 2 serves to illustrate the salient features of the profiling system. Situations can arise whereby the form of the trace is not a straight line, but elliptical. This is caused by a time phase-shift between the two signals. Details related to this phenomenon will not be given here. A comprehensive elucidation of this phenomenon as well as further details on the various aspects of the TE ratio profiling method can be found in Beyer (1977). For examples of case histories in which this method has been used successfully, the reader is referred to Beyer (1977) and Hoover and others (1981) and several references cited therein.

Audio-magnetotelluric method

The audio-magnetotelluric (AMT) method utilizes the natural multi-frequency electromagnetic energy described previously as its source. The inherent advantage of using natural sources instead of man-made artificial, or so-called controlled sources, is the relative ease in obtaining data. To survey large areas using a controlled source would require an inordinate amount of time, effort, and power to provide a near plane-wave electromagnetic field. On the other hand, the sometimes erratic behavior of the signal strength, direction of propagation, and frequency content of the natural signals can be an annoyance. However, the trade off is clearly in favor of using these natural signals as a source. At frequencies above 10 kHz, the signals produced from man-made transmitters in the very low frequency range (VLF) between about 11 kHz to 27 kHz are also used in AMT surveys.

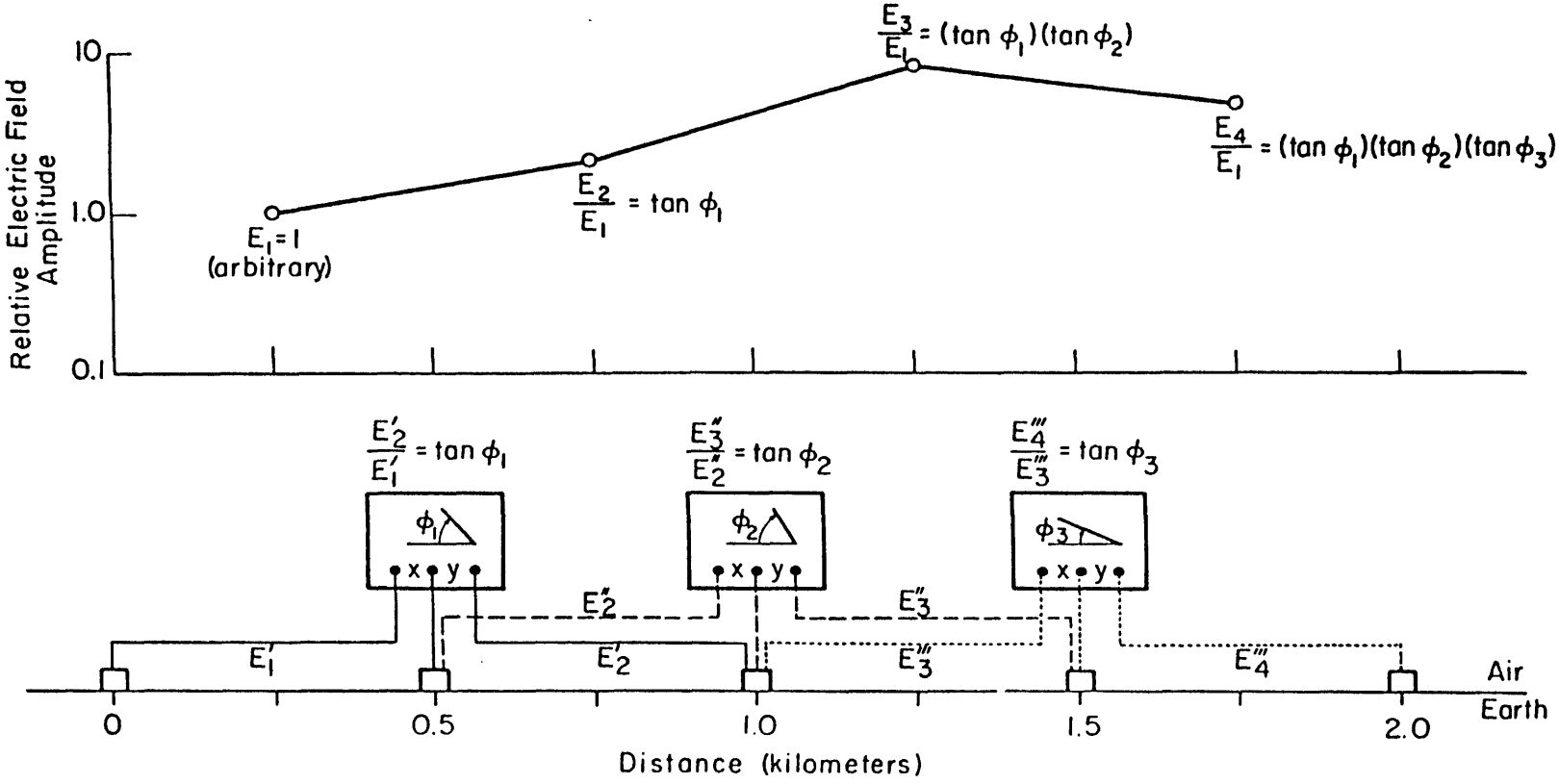

Figure 2.--A schematic presentation of three successive E-field ratio telluric recording stations and the data reduction technique (modified after Beyer, 1977).

The AMT method is well established and has been thoroughly described (see, for example, Strangway and others, 1973; Vozoff, 1972). For our purpose here, it is sufficient to know that the scalar apparent resistivity, ρa, is given by:

$$\rho a = 0.2T \left| \frac{E_x}{H_y} \right|^2 \qquad (1)$$

where T is the period (inverse of frequency) and E_x and H_y are the orthogonal and horizontal components of the electric and magnetic fields, respectively. Thus, to determine the apparent resistivity at a given frequency, one simply measures the ratio of these two electromagnetic components. As in other types of resistivity measuring systems, the apparent resistivity will be equal to the true resistivity if the medium has a uniform resistivity both laterally and vertically to distances that are larger than that which can be sensed by the system. Unlike d.c. measurement, however, the depth to which an alternating current electromagnetic wave travels is a function of its frequency and the resistivity of the medium. The amount of attenuation, or skin depth, δ, in meters, is an approximate measure of the exploration depth and is given by:

$$\delta = 503 \left(\frac{\rho}{f} \right)^{1/2} \qquad (2)$$

where ρ is the resistivity in ohm-m and f is the frequency in Hz. Formally, the skin depth is defined as the depth at which the amplitude of the signal has attenuated to 1/e (1/2.718) of its magnitude at the surface. Thus, by measuring the apparent resistivity at various frequencies, one can sense the resistivity distribution as a function of depth. In this manner, a resulting set of measurements over a range of frequencies at one location will provide a depth-sounding data set in approximately the same way as in progressively expanding the distance between the current and potential electrodes in d.c. resistivity sounding methods. For a horizontally stratified medium, an apparent resistivity is calculated as a function of frequency whose value is affected by the combined effects of the various layer resistivities and thicknesses, with the higher frequencies being responsive to the shallow section and the lower frequencies being progressively more responsive to the deeper parts of the section. In areas that are not electrically isotropic, in which large lateral contrast in resistivity occur locally, the measured values at varying azimuths of the orthogonal E and H fields will not be identical. That is, $E_x/H_y \neq E_y/H_x$. Details of the various responses for such electrically anisotropic situations are amply documented in the literature (see, for example, Pound and others, 1973; Strangway and Vozoff, 1970).

Nevertheless, the relative simplicity and effectiveness of measuring the scalar (versus the tensor) resistivity in two directions (E_{N-S}/H_{E-W} and E_{E-W}/H_{N-S}) as made in these studies has proven to be generally adequate for the purpose of developing geoelectric sections on a sub-regional reconnaissance scale.

The AMT as well as the TE systems used in this study were designed and fabricated by the USGS inasmuch as no suitable systems are available through the commercial market. Basic details of the AMT system are thoroughly described by Hoover and others (1976). Briefly, the electric field sensors consist of two 25-m length wires connected to three non-polarizing electrodes that are oriented in an L-shaped horizontal array to measure the N-S and E-W electric-field components. The corresponding magnetic field sensors consist of ferrite cores upon which are wound several hundred turns of wire. These induction coils are rigidly mounted at right angles to each other in a fiberglass flat box that is approximately 50 cm square and 10 cm deep. The box is partially buried in the surface soil to reduce noise induced by wind and is oriented north-south and east-west. The signals from these sensors are fed into a preamplifier and then to the main receiver via a 30-m length coaxial cable. The main receiver basically consists of high-gain amplifiers and band-pass filters for selectively tuning the receiver at 16 discrete frequencies that are logarithmically spaced from 4.5 Hz to 27 kHz. The outputs of the four channels (E_{N-S}, E_{E-W}, H_{N-S}, and H_{E-W}) are fed to two 2-channel high-frequency response, hot-pen chart recorders for displaying the shape and amplitude of the discrete spike-like signals. The average time in which to set up the system and record these data is approximately one hour (not including travel time to a receiving site). Accordingly, six to eight stations can be occupied in one day given favorable signal strengths and logistical factors.

Reduction of the acquired data is usually accomplished back at the field camp or office. Our data reduction system includes a hand digitizer whose output is connected to a minicomputer. The amplitude of the spike-like signals that were recorded on the chart paper are hand picked on the digitizer. These values are automatically entered into the computer that contains a program (C. L. Long, unpub., 1982) for computing the apparent resistivities according to equation (1). For each frequency and direction, as many as 20 samples are picked from the charts. The computer then calculates the average value from all the samples and its corresponding standard error. Good coherent data will typically have standard errors of less than 10 percent. Depending on circumstances, values up to 20 percent are generally acceptable. The reduced average values of apparent resistivity are stored in the computer and when all the available values have been entered for the various frequencies, the computer prints

out a log-log plot of these values versus frequency. From these data, an inversion model of the geoelectric section (resistivity versus depth) is generated using a relatively straightforward technique developed by Bostick (1977). The Bostick technique is very effective and fast for obtaining a general impression of the geoelectric structure from the sounding data. The technique, however, produces only an approximate solution and assumes that the structures are horizontally layered (electrically isotropic). The idealization of no lateral variation in the vicinity of a sounding often may not apply. Therefore, this technique is best used for first-order interpretations, which can be modified later by further analysis, if warranted or necessary. Through the final process of inversion, a geoelectric cross section can be constructed, particularly where measurement stations are located along linear traverses. The nature of these final products will be self evident in the following sections.

RESULTS AND DISCUSSION

Meshaheed area

The initial electromagnetic studies were carried out in a small region within the Meshaheed district (fig. 3; MODS 1266). An approximate east-west traverse, about 7.5 km in length, was established across an area that contains several geologic structures and mineralogic features of interest (fig. 4). The principal features include a small felsic pluton that is intruded into Murdama clastic rocks and is argillically altered and cut by a quartz-vein stockwork containing small amounts of molybdenum. A quartz-stibnite-gold vein or vein system also strikes through this pluton. This pluton is surrounded by a complex of sub-volcanic basalt(?) (dolerite?) that intrudes the Murdama metasedimentary rocks, that, in turn, is intruded by small stocks of granodiorite and plagioclase porphyry. The basaltic rocks are hydrothermally altered and a zone approximately 1 km long and several hundred meters wide contains zones of silicification, pyritization, carbonatization, and argillization. Much of this area, however, is covered and, therefore, the areal and depth extent of the zone of alteration is unknown. The exposed altered zone is anomalous in concentrations of gold, arsenic, and antimony.

A series of granodiorite plutons are exposed several kilometers to the west of the intrusive complex. Numerous ancient gold-mine workings abound within the Murdama metasedimentary rocks in a contact aureole around parts of these plutons. Two small plugs of granodiorite are locally hydrothermally altered and contain some quartz-stibnite-gold-bearing veins.

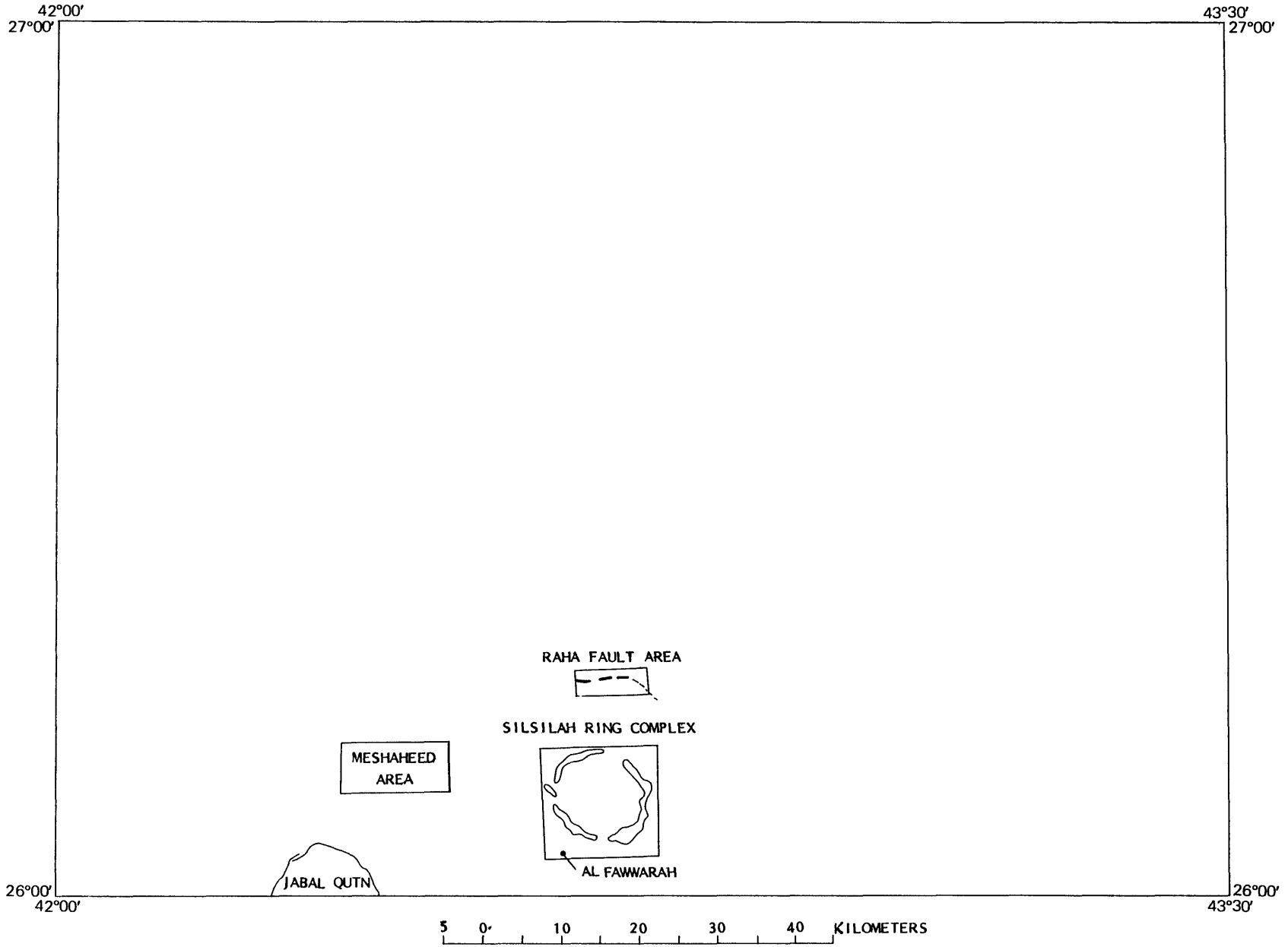

Figure 3.--Index map of the Jabal Hibshi quadrangle, 26F, showing the locations of the Meshaheed, Silsilah, and Raha-fault areas where electromagnetic studies were made.

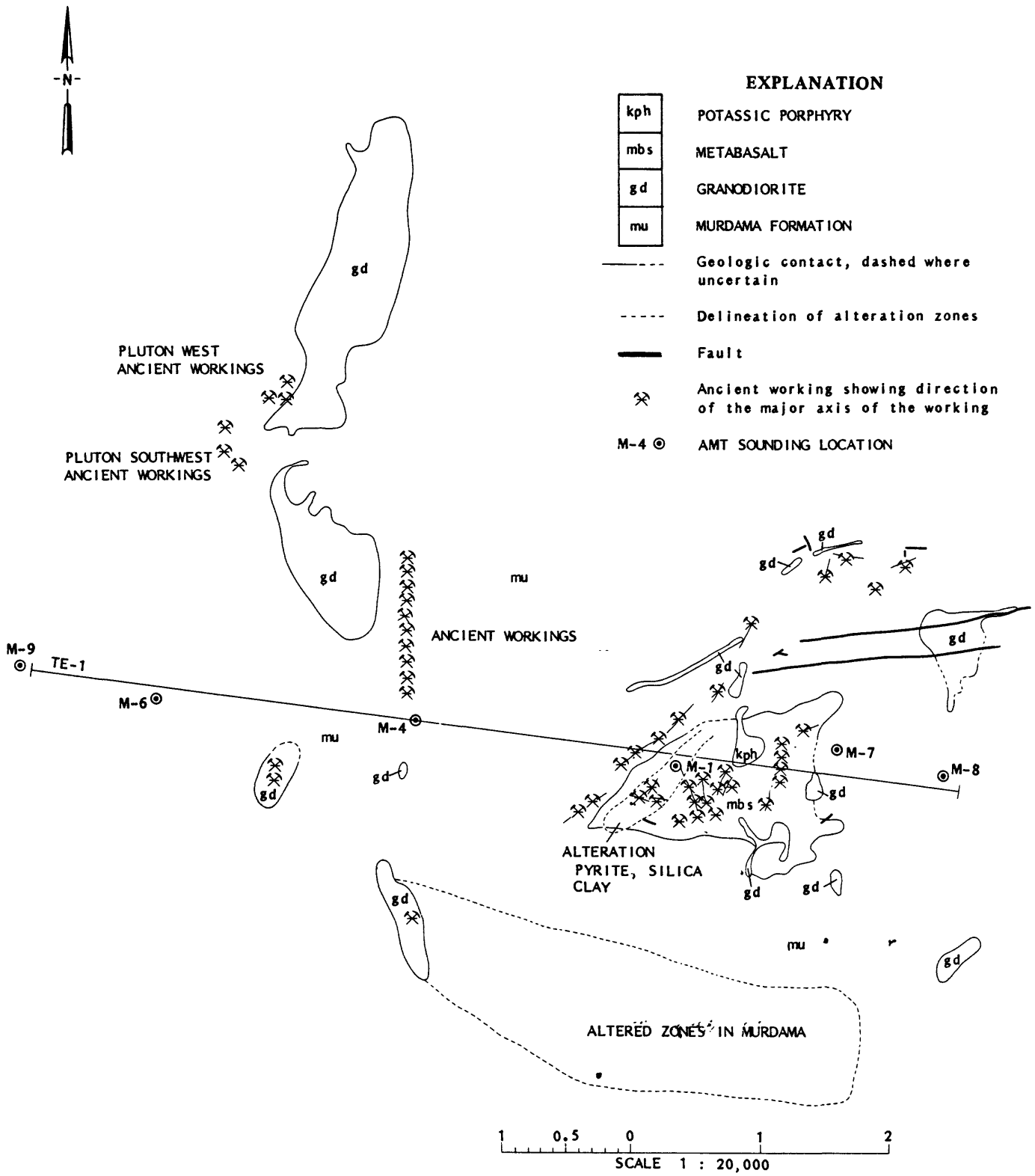

Figure 4.--Generalized geologic map of the Meshaheed area (modified after C. W. Smith, written commun., 1983) showing location of traverse TE-1 along which TE and AMT measurements were made.

Large zones of argillic alteration in the Murdama metasedimentary rocks extend from Jabal Qutn, about 10 km to the south of the Meshaheed district, to about 1.5 km south of the area of the traverse. These zones are distinguished by color contrast -- tan to reddish-brown in contrast to the dark-gray color of the unaltered metasediments. Pyrite is present in small amounts in most parts of these altered zones and geochemical sampling has indicated low values of molybdenum.

A TE-ratio profile was made along the traverse using 250-m length bipoles. A plot of the resulting relative E-field amplitudes is shown in figure 5. Included in this figure is a geoelectric cross section derived from the interpreted resistivity distribution as a function of depth from the AMT soundings made at the station locations so indicated. The resistivity distribution is displayed in contour form in which the contour values are logarithmically spaced at five divisions per decade. It is seen that there is generally a good correspondence between the relative E-field amplitudes and the geoelectric cross section derived from the AMT results. The clearest correlation occurs in the vicinity of AMT station M-1 in which the relative E-field amplitudes decrease gradually on the west side of a broad low-resistivity zone and increase more sharply on its east side. The contoured resistivity cross section follows the same trend. This low resistivity zone, about 2 km in width, and extending to depths in excess of several kilometers, coincides with the surface extent of the exposed altered sub-volcanic complex. The most electrically conductive part of this area coincides exactly with the location of the highly altered felsic pluton exposed at the surface. The low resistivities associated with the altered rocks undoubtedly are caused by their relatively higher content of clay minerals resulting from alteration processes in contrast to the unaltered igneous or metasedimentary rocks in the surrounding area. It is significant to note that the highest relative E-field amplitudes occur at, and immediately to the west of, AMT station M-4 and probably reflect subsurface extensions of the relatively large granodiorite plutons that outcrop approximately 1 km to the north and south of the traverse. The pattern of the cross section in this area also suggests a corresponding high-resistivity zone at depth. The cause of the short-wavelength local high relative E-field amplitude near the westernmost end of the profile is unknown, but possibly is related to a small, shallow granodiorite plug. Near the eastern end of the traverse, centered about 200 m west of the AMT station M-8, the relative E-field amplitude profile shows a zone of extremely low resistivity. Although the AMT cross section does not indicate a proportionately anomalous conductive zone, the AMT data at M-8 does, in fact, indicate that lower resistivities extended to deeper depths than at M-7. If this conductive feature has steeply dipping sides, then the approximately ten-fold difference in the relative E-field amplitudes measured

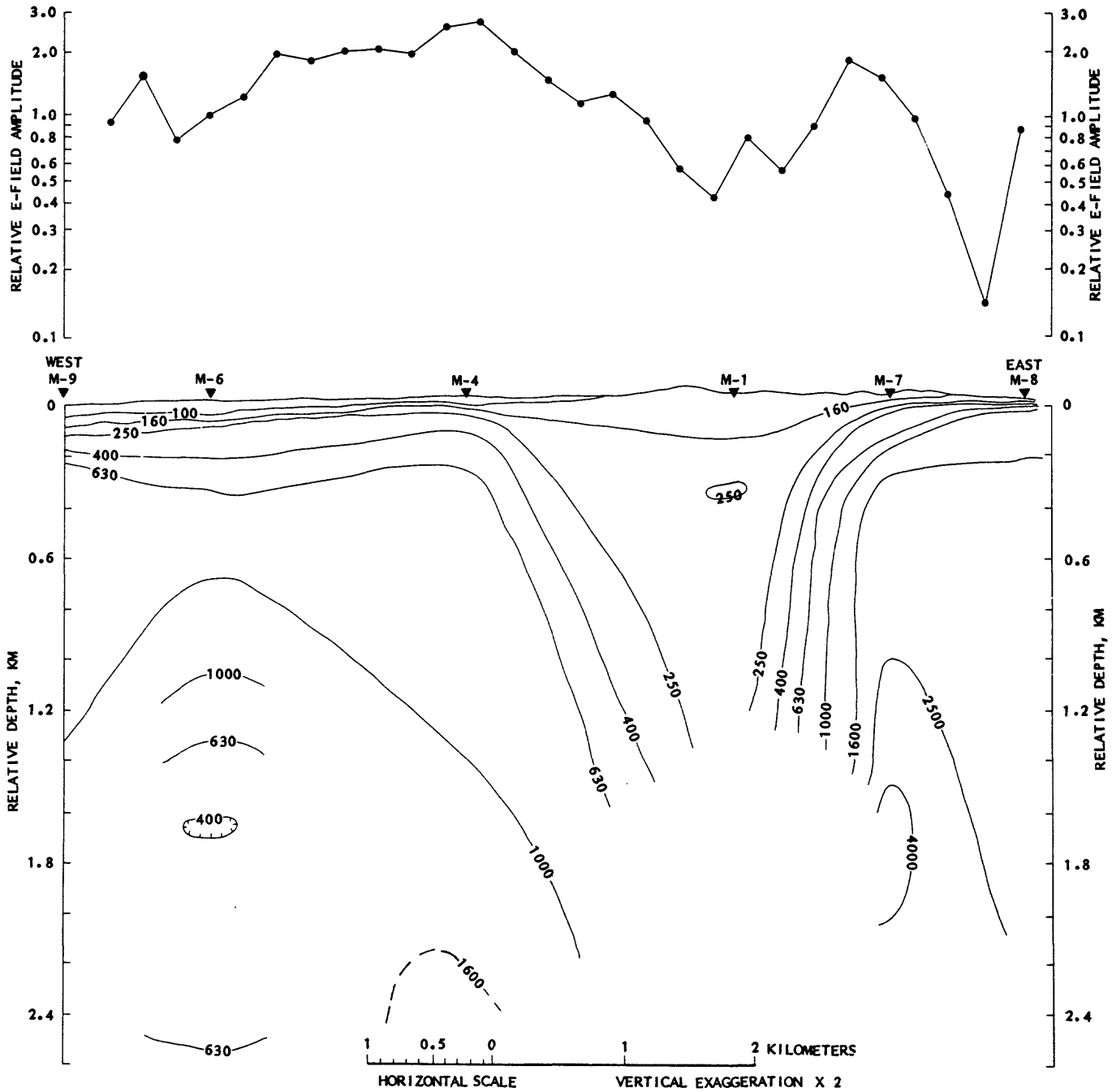

Figure 5.--Results from the TE and AMT surveys made along transect shown in figure 4.

between AMT stations M-7 and M-8 would require about a 100 to 1 contrast in the resistivities beneath the two areas. This estimate is based on the following relationship between the ratio of the relative E-field amplitudes (E_1/E_2) and the corresponding resistivity ratio (ρ_1/ρ_2) across a vertical contact:

$$\frac{E_1}{E_2} = \left(\frac{\rho_1}{\rho_2}\right)^{1/2} \qquad (3)$$

Further detailed geological studies in the area may be able to reconcile the cause of this conductive anomaly. It is possible that this area is underlain by similar, if not more intensely, altered rocks than the exposed felsic pluton in the vicinity of AMT station M-1.

The average resistivity value of the unaltered metasedimentary rocks in the area along the traverse appears to be about 500 to 600 ohm-m. If this is so, then their thickness to the west of AMT station M-4 would be about 500 m and much thinner (several hundred meters or less) to the east of AMT station M-7.

It is apparent from this initial study that large resistivity contrasts exist between the three principal rock types encountered in this area. The major controlling factor for these contrasts most likely is associated with their clay-mineral content. Clay minerals possess large cation-exchange capacities that result in increasing the ion concentration available for conduction through the pore fluids. This phenomenon is often referred to as "double-layer" conductivity (Keller and Frischknecht, 1966, p. 24). As the interstitial or intercrystalline porosities of these rocks are very low, contributions from electrolytic conduction through open water-filled fractures would also be a factor, but may be only secondary in importance here. Accordingly, unaltered (specifically, non-argillic) igneous rocks have fairly high resistivities; the metasedimentary rocks of the Murdama group have intermediate values of resistivity as these rocks generally contain up to several percent by volume of clay minerals (P. L. Williams, USGS, personal commun., 1983); and highly altered rocks, containing abundant clay minerals, have very low values of resistivity. These generalizations were reinforced by the results from studies subsequently made in the area of the Silsilah ring complex located about 25 km to the east of the Meshaheed district.

Silsilah area

The predominant geologic structural feature in the Silsilah area is a circular ring complex, about 14 km in diameter, called Jabal as Silsilah (fig. 3). A generalized

geologic map of this area is shown in figure 6. The ring complex is unusual because it is composed of both peraluminous and peralkaline intrusive phases. Several greisenized patches of Fawwarah monzogranite crop out inside the southwest part of the ring structure. Two of these outcrops are thoroughly greisenized; these quartz-cassiterite-topaz-bearing greisens locally contain greater than two percent tin. These and other cupolas of monzogranite in the southwestern sector intrude the exposed, or near-surface, weakly metamorphosed graywacke sandstones of the Murdama group. Further details on the structural and mineralogic setting of this area may be found in du Bray (*in press*).

The primary objective of our electromagnetic studies in this area was to attempt to determine the gross nature of the subsurface geology within the ring complex. Such information could provide further insight for developing conceptual ore occurrence models for this type of geologic setting and in similar settings elsewhere within the Kingdom.

Two electromagnetic traverses were established across the ring complex; one oriented N. 80° W. that approximately bisected the complex (labelled TE-1 in fig. 6) and the other oriented N. 45° E. through the east-central portion of the complex (labelled TE-2 in fig. 6). Similar to the studies made in the Meshaheed district, TE-ratio measurements were made along these traverses, but using 500-m length bipoles instead of the 250-m length bipoles as used previously at Meshaheed. AMT soundings were also made at approximately 2-km intervals along, or near, these profiles. The results from these surveys are shown in figures 7 and 8 and are presented in the same manner as those obtained from the Meshaheed district. These results reveal some interesting characteristics of the subsurface geology. The relative E-field amplitude profiles and the geoelectric cross sections derived from the AMT sounding data are mutually compatible. At the west end of the N. 80° W. profile (fig. 7), both the E-field and AMT data reflect the high resistivities associated with the exposed ring dikes. Immediately to the east of this structure, in the vicinity of AMT station F-6, both data sets reveal an unusually high-conductivity zone of several kilometers in width and depth extent. The attitude of this well-defined feature appears to dip steeply towards the inner complex as suggested in the cross section. The highest resistivities along this traverse are defined between the interval from about 1 km east of AMT station F-5 to about 1 km west of AMT station F-2. In contrast to the western side of this complex, the eastern side is only moderately to weakly conductive as seen from both the relative E-field amplitude profile and the geoelectric cross section. The dikes that form the eastern side of the complex are much less resistive than those on the western side. In the vicinity of the felsic dike that trends in a northeast-southwest direction through

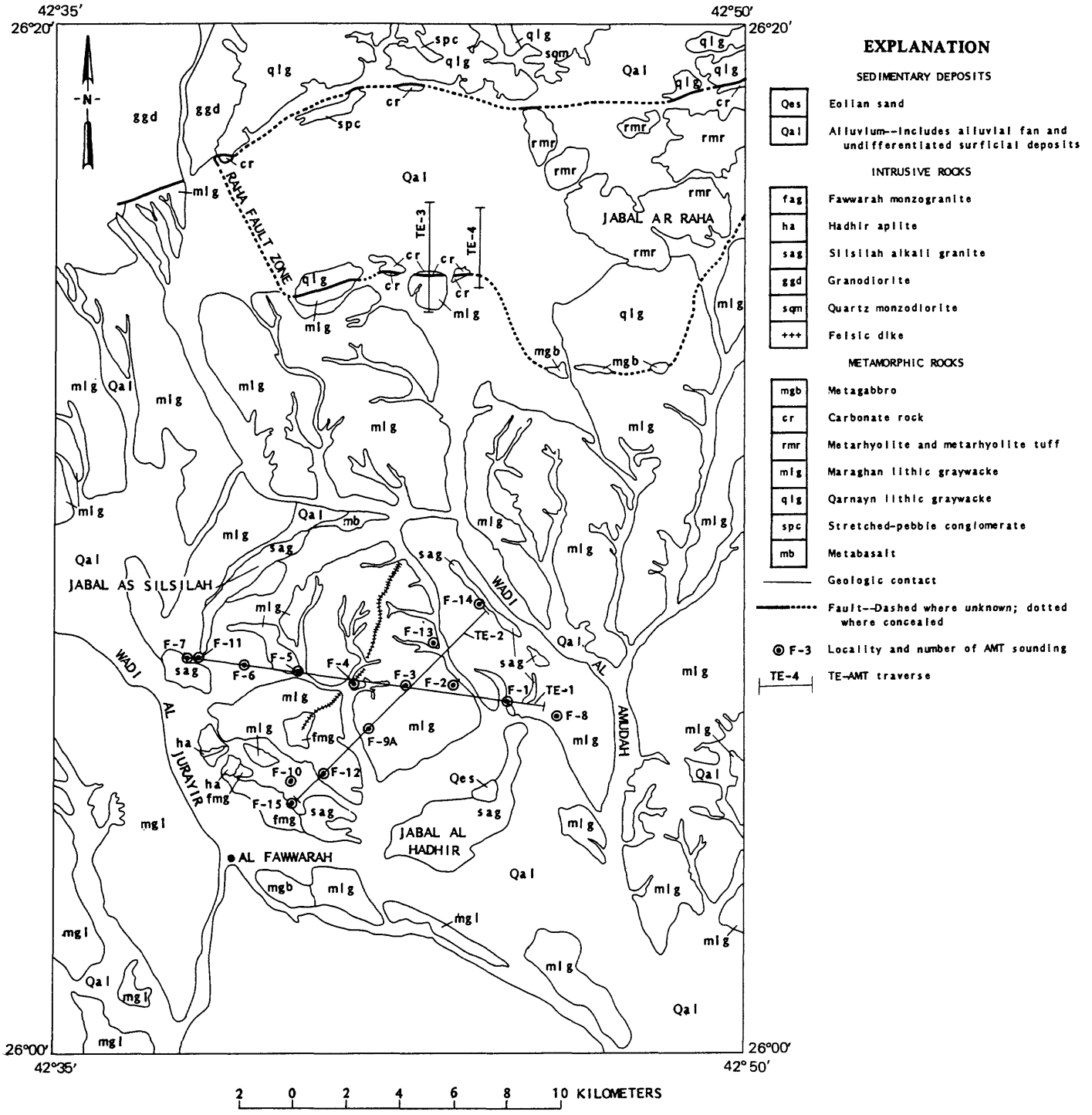

Figure 6.--Simplified geologic map of a part of the Jabal as Silsilah quadrangle, 6/42 D, (modified after du Bray, *in press*). Also shown are the locations of four traverses along which TE and AMT measurements were made.

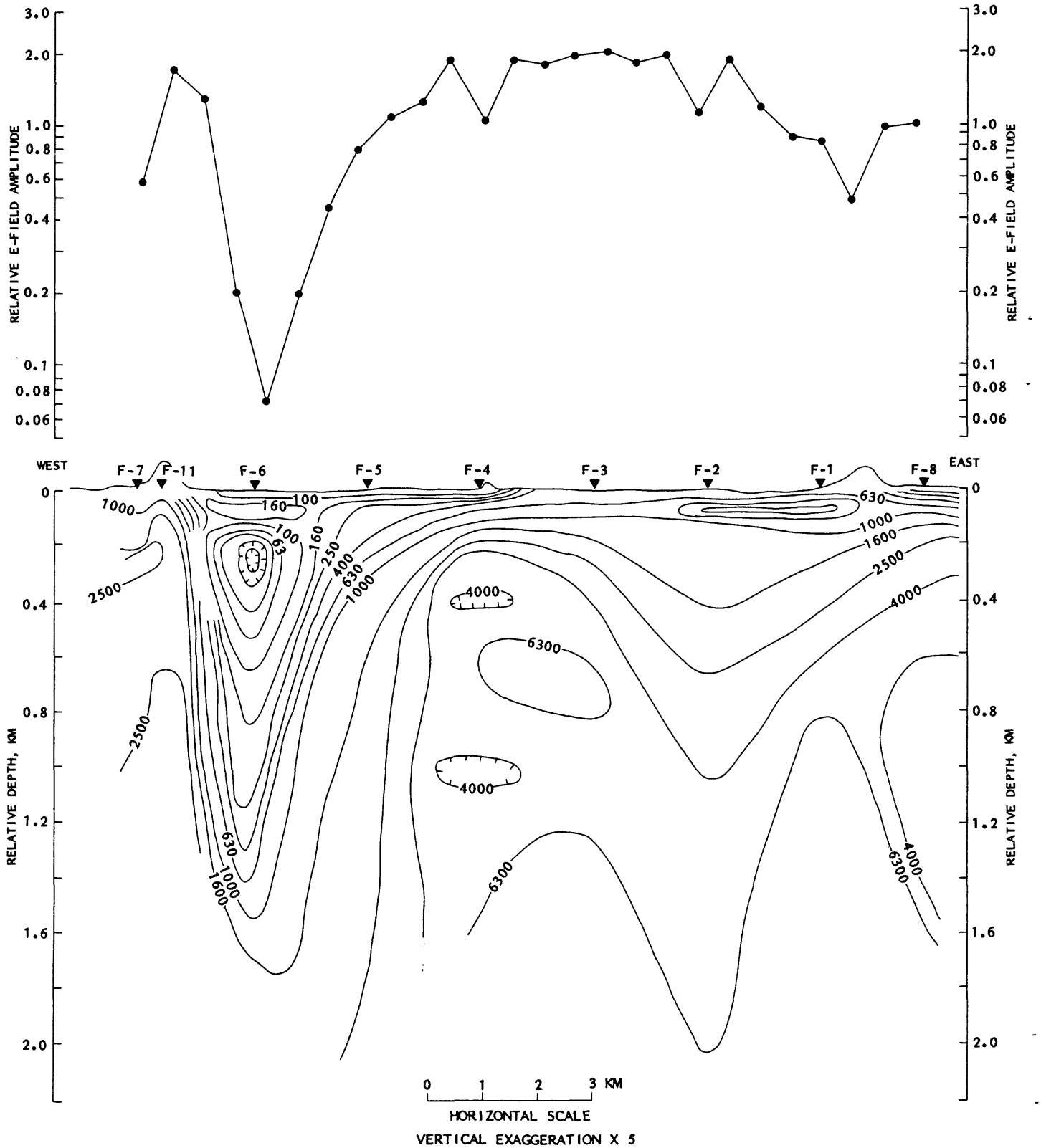

Figure 7.--Results from the TE and AMT surveys made along traverse TE-1 shown in figure 6. Inverted solid triangles labelled F-1, etc., are locations of AMT stations.

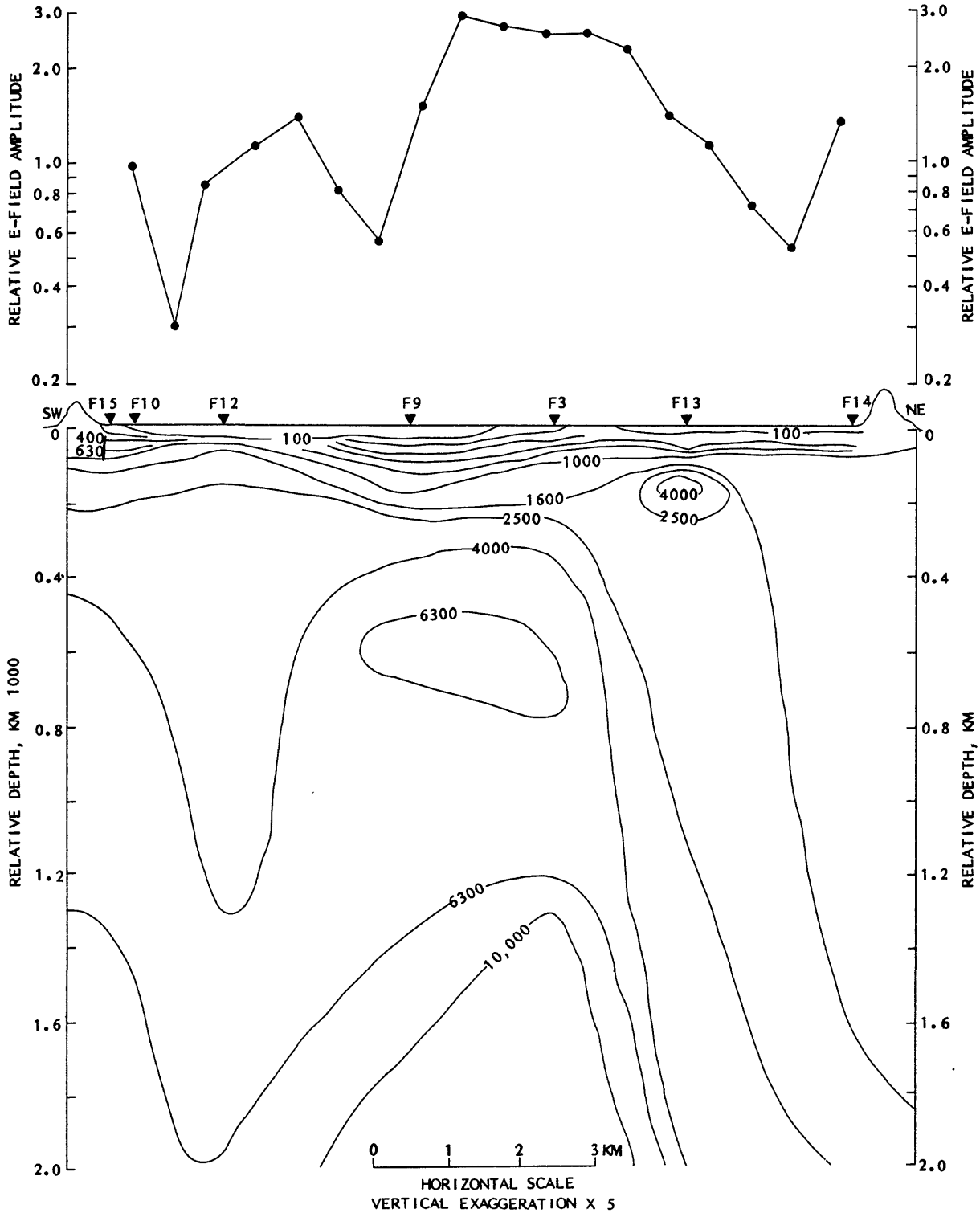

Figure 8.--Results from the TE and AMT surveys made along traverse TE-2 shown in figure 6.

the central portion of the ring complex (near AMT station F-4 on the N. 80° W. traverse), the relative E-field amplitude profile detected a thin, moderately conductive zone. The narrow width of this feature is not resolved from the AMT data. This local low-resistivity zone may not result from the electrical properties of the dike itself, but possibly from a narrow fracture zone that may be nearly coincident and associated with the dike. By extrapolating the approximate 500 to 600 ohm-m resistivity value for the weakly metamorphosed sedimentary rocks of the Murdama group suggested by the studies made in the Meshaheed district, the thickness of these rocks within the complex appears to be much thinner (less than 200 m).

The results from the N. 45° E. traverse (labelled as TE-2 in fig. 6) have the general characteristics of those obtained from the N. 80° W. traverse, with some notable differences (fig. 8). The relative E-field amplitudes near the southwest outcrop of the ring dike indicate the presence of a moderately conductive zone of narrow width between AMT stations F-15 and F-12. The geoelectric cross section in this vicinity also shows that this zone is only moderately conductive at depth relative to the adjacent rocks. The broad low-resistivity zone, centered near AMT station F-9, is manifested by low relative E-field amplitudes and a corresponding thickening of the near-surface moderately conductive zone shown in the cross section. Beneath this zone, and extending northeast to about AMT station F-13, a deeper seated, very high-resistivity zone exists. Further to the northeast, a characteristically conductive zone lies toward the inside periphery of the exposed ring dikes as indicated by the E-field data. The data obtained at AMT station F-14 suggest that rocks of moderate resistivity (1,600 ohm-m) extend from near surface to depths in excess of one kilometer. This zone is less conductive than the corresponding zone on the west side. However, it is more conductive than the peripheral zones on the southwest or east sides of the complex.

The results obtained from the studies made in this area provide information that should be very useful in modeling the form of the present substructure as well as in gaining insights into its evolution. In the following, we summarize the most significant aspects of these results for consideration in translating them into a viable geologic model:

1. The extremely low-resistivity zone defined on the western side of the complex is probably related to intensely altered and (or) fractured rocks resulting from shearing and (or) hydrothermal processes. The lateral extent of this zone was not defined by these limited studies. However, the degree of alteration or fracturing appears to be much less in the vicinity of the southwest part of traverse TE-2 and, therefore, the highly altered zone is probably limited to the western sector.

2. The low-resistivity zones defined towards the ends of the two traverses appear to be related to ring fracturing along the periphery of a buried stock. Their values of average resistivity, however, are quite different. They are qualitatively ranked from low to high as follows: west, northeast, southwest, and east. This ranking of increasing resistivity is in accord with some field observations and petrographic studies of the nearby outcrop ring dikes made by Edward du Bray (oral commun., 1983). His studies indicate that these rocks are most fractured on the west side, intermediately fractured on the northeast and southwest sides, and least fractured on the east side. The pattern of clay alteration is assumed to follow accordingly. The extrapolation of these observations to the possible conditions in these peripheral zones may not apply, but does appear to be compatible with the geoelectric results.

3. The high resistivity zone (defined here as 4,000 ohm-m or greater) that lies at depth within the central part of the complex most likely reflects the inner core of the ring complex. These large resistivity values require that the core rocks be very competent (having low total porosity) and containing little or no clay minerals. The general increase in resistivity with depth suggests that the rocks correspondingly become progressively denser (less porous) with depth.

4. Other local and broader variations in the resistivity distribution shown in the geoelectric cross sections may be meaningful and should be considered in developing compatible geologic models. On the immediate flanks of the so-called inner core, as an example, the relatively shallow and high-resistivity zones shown in the vicinity of AMT station F-13 and between AMT stations F-2 and F-1 may be related to occurrences of shallow intrusions fed from the central core (i.e., cupolas). Also, the relatively lower resistivities associated with the core (between approximately 1,000 ohm-m to about 4,000 ohm-m) may reflect transitional phases in the main intrusive stock.

Raha fault area

In mapping the general geology of the Jabal as Silsilah quadrangle, du Bray has identified a major fault zone (Raha fault zone). A portion of the outcropped and inferred location of this zone is shown in figure 6. A detailed description of this tectonic feature have been described by du Bray (in prep.). Two TE profiles were made across a section of this feature to determine if the rocks on either side indicated any differences in their gross electrical properties. One traverse was established in a north-south direction normal to the outcropped fault trace (traverse TE-3 in fig. 6) and the other was established parallel to, and approximately, two

kilometers to the east of traverse TE-3 (traverse TE-4 in fig. 6). The resulting profiles of the relative E-field amplitudes are shown in figure 9. The relative E-field amplitude profile along traverse TE-3 clearly indicates an abrupt and large contrast in the electrical resistivity of the rocks on either side of the fault zone. The change in the relative E-field amplitudes is about 4 to 1, being larger on the north side. According to equation (3), the resistivity ratios may be as large as 16 to 1. The outcropped, or near-surface rocks, on the south side of this fault are weakly metamorphosed graywackes whereas the predominant rock type exposed on the north side is of the same general type except that these rocks have a higher rank of metamorphism (du Bray, oral commun., 1983). If this is so, then the relatively large resistivities of the graywackes on the north side may result from the conversion of original clay minerals into micas (principally biotite). Void of any clay minerals, these rocks would be expected to have resistivities similar to unaltered igneous rocks (i.e., greater than 6,000 ohm-m).

The results from the profile along traverse TE-4 do not show any significant changes across the inferred extension of the fault zone to the east (fig. 9). Two explanations are plausible: 1) the subsurface extension of the fault is not correctly portrayed; or 2) the angle of incidence between the profile and the strike of the fault is too acute for this method to detect any change. This method is most effective when the profile is made nearly perpendicular to the assumed strike of a feature. For traverses made at acute angles over structures that locally have large resistivity contrast, the telluric currents may be channeled in such a way as to give a false or no indication of the underlying geoelectric structure. It is noteworthy that in attempting to measure E-field ratios immediately to the south of these profiles, the recorded plots on the X-Y recorder produced large-amplitude ellipses whose major axis was oriented in a predominantly north-south direction. Explanations for such a behavior of the relative telluric voltages in this type setting can be found in Beyer (1977). Briefly, this behavior suggests that this area contains relatively high conductive (altered?) zones within the graywackes. This general area contains evidence of ancient gold workings from quartz veins. Topical studies, using controlled-source electrical methods, could delineate these local conductive zones that would be helpful in further detailed geologic and geochemical studies of this area.

CONCLUSIONS

The results from these limited electromagnetic studies and their corresponding geologic implications presented herein clearly demonstrate the appropriateness of these type

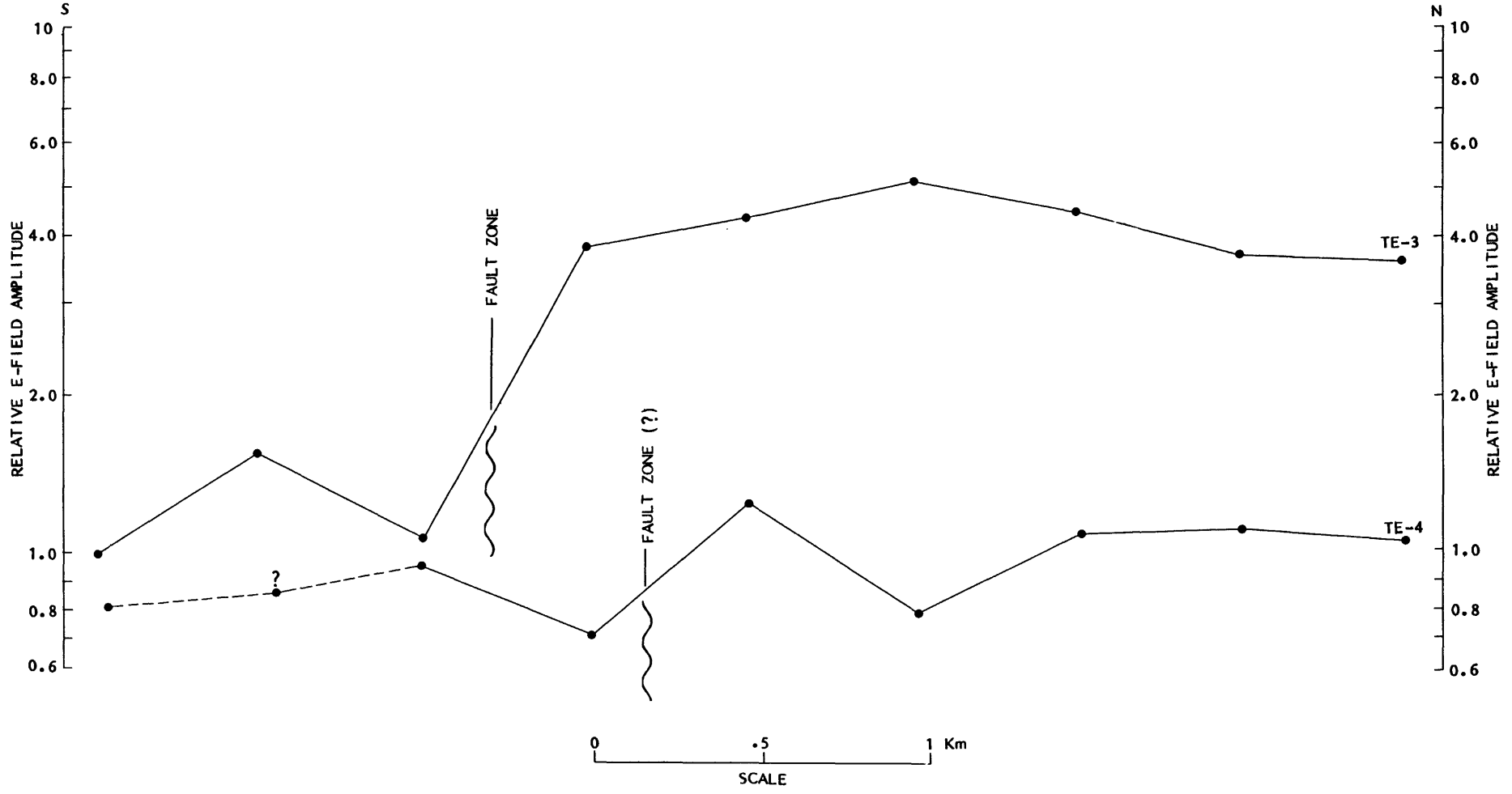

Figure 9.--TE profiles along traverses TE-3 and TE-4 shown in figure 6.

studies to the mission's primary goal of assessing the mineral resource potential within the Kingdom.

The relatively short time in which these data were acquired, processed, and interpreted (about two weeks) attest to not only their appropriateness, but also to their efficiency in providing timely and substantive structural and mineralogical information in the third dimension. This type of information could be invaluable particularly to the field geologist. Having been made aware of any anomalous features revealed by these types of electromagnetic surveys conducted in his general area of study, the geologist could efficiently utilize his time and efforts in studying these specific areas in more detail in conjunction with other available information (for example, aeromagnetic and geochemical data).

Whereas quantitative interpretations from AMT measurements are generally appropriate, only qualitative interpretations from the TE field ratio results are generally warranted. This is because of the lack of complete information of the total electromagnetic field at the earth's surface (i.e., only one component of the electric field is recorded and the corresponding orthogonal magnetic field component is not). Nevertheless, this method has several features that make it appropriate for sub-regional scale investigations.

1) Anomalies can be defined that may be followed up by other more detailed geophysical and geochemical studies.

2) Extensions of known geologic, geochemical, and other geophysical anomalies may be rapidly traced to decide if additional surveys are needed or warranted.

3) The results may be used to dictate the location and spacing of follow-up AMT surveys. Thus, attention could be focused on avoiding the siting of AMT stations along high gradients of the E-field that might imply a three-dimensional structure and thereby cause difficulty in interpreting the AMT sounding data.

4) The results could also be used in dictating the AMT site-spacing interval for adequately defining an anomaly and, thereby, avoiding over sampling.

DATA STORAGE

Data file USGS-DF-04-8 (Flanigan and Zablocki, 1984) has been established for the storage of data used in this report.

No entries or updates have been made to the Mineral Occurrence Documentation System (MODS) data bank.

REFERENCES CITED

Bostick, F. X., 1977, A simple almost exact method of MT analysis, in Ward, S. H., ed., Workshop on electrical methods in geothermal exploration: Univeristy of Utah, Salt Lake City, UT, 84112, p. 175-183.

Beyer, J. H., 1977, Telluric and D.C. resistivity techniques applied to the geophysical investigations of Basin and Range geothermal systems: University of California, Lawrence Berkeley Lab Report LBL-6328.

du Bray, E. A., in press, Reconnaissance geology of the Jabal as Silsilah quarangle, sheet 26/42 D, Kingdom of Saudi Arabia: Saudi Arabian Deputy Ministry for Mineral Resources map series, 52 p.

Flanigan, V. J., and Zablocki, C. J., 1984, Supporting data for an evaluation of the applicability of the telluric-electric and audio-magnetotelluric methods to mineral assessment on the Arabian Shield: Available from Saudi Arabian Deputy Ministry for Mineral Resources Data-File USGS-DF-04-8.

Hoover, D. B., Frischknecht, F. C., and Tippens, C. L., 1976, Audio-magnetotelluric soundings as a reconnaissance exploration technique in Long Valley, California: Journal of Geophysical Research, v. 81, p. 801-809.

Hoover, D. B., Broker, M. M., and Stambaugh, T., 1981, E-field ratio telluric survey near the Big Maria Mountains, Riverside County, California: U.S. Geological Survey Open-File Report 81-961, 15 p.

Hoover, D. B., Chornack, M. P., and Broker, M. M., 1982, E-field ratio telluric traverses near Forty Mile Wash, Nevada Test Site, Nevada: U.S. Geological Survey Open-File Report 82-1042, 15 p.

Keller, G. V., and Frischknecht, F. C., 1966, Electrical methods in geophysical prospecting: Pergamon Press, New York, 517 p.

Pound, J. G., Bostick, F. X., Jr., and Smith, H. W., 1973, An experimental system for audio-magnetotelluric measurements: Austin, University of Texas, Electrical Research Center, Technical Report no. 151.

Strangway, D. W., Swift, C. M., Jr., and Holmer, R. C., 1973, The application of audio-frequency magnetotellurics (AMT) to mineral exploration: Geophysics, v. 38, no. 6, p. 1159-1175.

Strangway, D. W., and Vozoff, K., 1970, Mining exploration with natural electromagnetic fields [with French abstract], in Mining and groundwater geophysics, 1967: Canada Geological Survey Economic Geology Report 26, p. 46-50.

Vozoff, Keeva, 1972, The magnetotelluric method in the exploration of sedimentary basins: Geophysics, v. 37, no. 1. p. 98-141.

APPENDIX

Explanation

In the following, a list of the computer-derived AMT sounding data obtained from these studies and the corresponding interpretations is presented in tabular form. The observed data (OBS-RES) represents a smoothed, best-fit curve obtained from the combined N-S and E-W sounding measurements. The calculated resistivities (CAL-RES) are the forward plane-wave values based on the results of an inversion calculation of the observed data using an algorithm developed by Bostick (1977). This is followed by a log-log plot of the data obtained from both the inverse and forward calculations for visual comparison. Also presented is a log-log plot of the final end product -- the resistivity distribution as a function of depth. It is from these plots that the geoelectric cross sections presented in this report were constructed.

Part A of this appendix includes the data obtained from the studies made in the Meshaheed area and Part B from those in the Silsilah area.

APPENDIX, PART A

MESHAHEED AREA

OUTPUT FROM BOSTICK

STA-ID M-1ANS
AMP INVER INPUT CURVE

LAYER NO.	RESISTIVITY	DEPTH
1	250.01	34.64
2	352.13	50.46
3	624.14	76.65
4	527.67	103.92
5	500.00	138.56
6	436.90	194.82
7	632.50	281.94
8	836.86	388.84
9	888.43	532.17
10	835.67	775.70
11	980.31	1119.30
12	1127.60	1517.90
13	845.41	1971.80
14	827.97	2746.70
15	814.99	3752.80
16	793.09	4829.90

OUTPUT FROM AMT-MT FORWARD

FREQ.	OBS-RES	CAL-RES	ANGLE
27000.00	250.00	246.27	40.58
14000.00	275.00	274.59	38.36
7500.00	340.00	314.45	37.67
4500.00	375.00	349.22	38.19
2700.00	400.00	377.78	39.26
1400.00	410.00	400.30	40.35
750.00	460.00	416.74	40.30
450.00	525.00	437.43	39.68
270.00	590.00	467.22	39.05
140.00	650.00	514.83	38.48
75.00	725.00	571.15	38.15
45.00	800.00	626.37	38.28
27.00	810.00	683.81	38.94
14.00	815.00	747.62	40.33
7.50	815.00	789.24	41.81
4.50	810.00	809.00	42.88

OUTPUT FROM PLOT

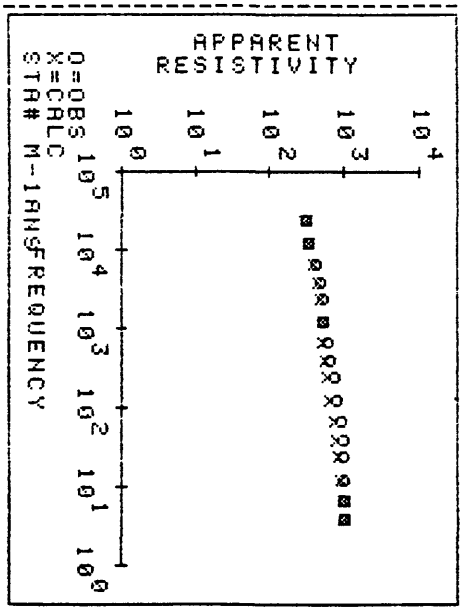

OUTPUT FROM BOSTICK

STA-ID M-1AEW
AMP INVER INPUT CURVE

LAYER NO	RESISTIVITY	DEPTH
1	25.00	10.95
2	105.93	18.26
3	137.86	29.39
4	98.27	40.87
5	67.43	53.67
6	104.99	80.50
7	115.95	117.58
8	150.92	162.78
9	167.35	224.50
10	198.30	340.17
11	219.50	500.56
12	225.50	678.82
13	209.61	903.33
14	188.56	1272.80
15	157.04	1713.90
16	170.01	2212.70

OUTPUT FROM AMT-MT FORWARD

FREQ.	OBS-RES	CAL-RES	ANGLE
27000.00	25.00	26.27	34.59
14000.00	36.00	33.65	31.95
7500.00	50.00	42.77	32.46
4500.00	58.00	49.79	34.09
2700.00	60.00	55.51	35.75
1400.00	70.00	61.39	37.06
750.00	80.00	66.92	37.31
450.00	92.00	72.33	37.03
270.00	105.00	79.08	36.53
140.00	125.00	90.31	35.89
75.00	145.00	104.09	35.60
45.00	160.00	117.52	35.82
27.00	170.00	132.24	36.55
14.00	175.00	150.47	38.30
7.50	170.00	163.13	40.38
4.50	170.00	169.11	41.93

OUTPUT FROM PLOT

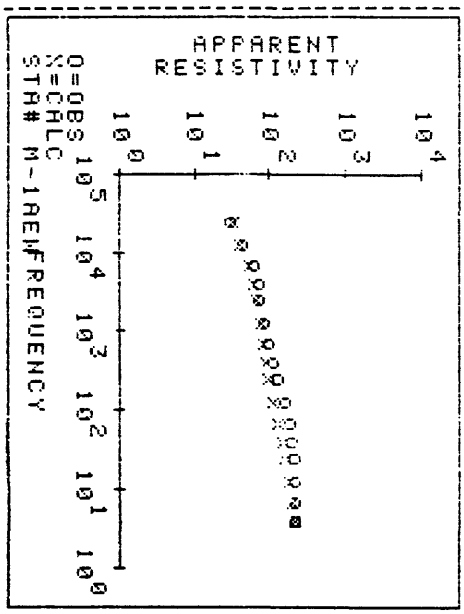

OUTPUT FROM BOSTICK

STA-ID M-4AAMP INVER INPUT CURVE

LAYER NO.	RESISTIVITY	DEPTH
1	60.00	16.97
2	84.51	24.72
3	138.11	37.18
4	176.21	52.31
5	288.15	75.90
6	273.90	117.84
7	472.97	185.90
8	377.15	257.37
9	836.87	379.47
10	893.29	608.51
11	838.00	915.47
12	1206.20	1303.50
13	1388.40	1846.10
14	2462.80	3012.00
15	3605.50	4929.90
16	4737.80	7099.30

OUTPUT FROM AMT-MT FORWARD

FREQ.	OBS-RES	CAL-RES	ANGLE
27000.00	60.00	58.78	41.13
14000.00	66.00	63.10	38.57
7500.00	80.00	70.56	36.13
4500.00	95.00	79.53	34.40
2700.00	120.00	91.59	32.98
1400.00	150.00	111.90	31.85
750.00	200.00	135.25	31.09
450.00	230.00	159.19	30.31
270.00	300.00	190.31	29.64
140.00	400.00	242.14	29.32
75.00	485.00	301.82	29.51
45.00	590.00	356.36	29.58
27.00	710.00	418.64	29.15
14.00	980.00	525.84	27.78
7.50	1350.00	681.20	26.35
4.50	1750.00	862.90	25.73

OUTPUT FROM PLOT

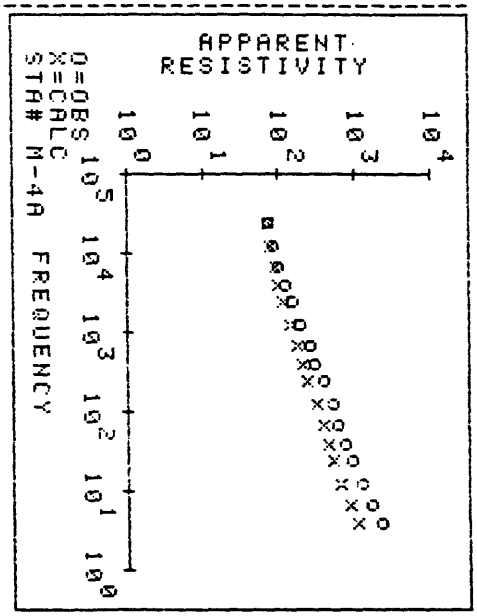

OUTPUT FROM BOSTICK

STA-ID M-6AMP INVER INPUT CURVE

LAYER NO.	RESISTIVITY	DEPTH
1	52.00	15.80
2	63.57	22.56
3	76.23	32.20
4	69.41	42.26
5	93.78	57.13
6	170.43	89.74
7	285.35	142.19
8	287.41	202.23
9	439.22	293.94
10	642.40	481.07
11	996.37	777.69
12	1249.20	1144.70
13	577.26	1517.90
14	685.51	2215.00
15	1600.20	3477.90
16	2006.10	5020.00

OUTPUT FROM AMT-MT FORWARD

FREQ.	OBS-RES	CAL-RES	ANGLE
27000.00	52.00	51.94	42.99
14000.00	55.00	54.35	42.21
7500.00	60.00	56.62	41.93
4500.00	62.00	57.71	41.47
2700.00	68.00	58.87	40.13
1400.00	87.00	63.15	37.23
750.00	117.00	71.81	34.19
450.00	142.00	82.56	31.90
270.00	180.00	97.38	29.63
140.00	250.00	127.40	26.86
75.00	350.00	174.14	25.70
45.00	455.00	224.91	26.49
27.00	480.00	278.54	28.30
14.00	530.00	341.68	30.19
7.50	700.00	406.61	30.46
4.50	875.00	478.09	30.07

OUTPUT FROM PLOT

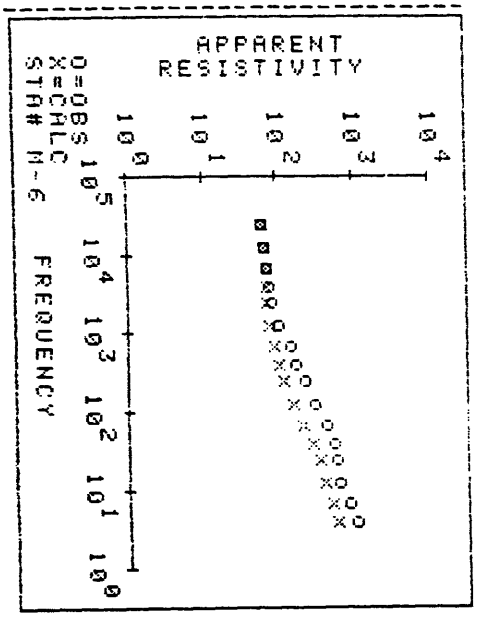

OUTPUT FROM BOSTICK

STA-ID M-7AMP INVER INPUT CURVE

LAYER NO	RESISTIVITY	DEPTH
1	130.00	24.98
2	315.41	39.08
3	468.91	60.95
4	572.12	87.36
5	501.63	121.00
6	723.94	188.79
7	1127.10	295.40
8	1858.80	435.98
9	1717.30	623.54
10	1760.40	962.14
11	2813.30	1498.80
12	4046.90	2179.90
13	4028.50	3098.40
14	3317.10	4614.30
15	2208.10	6269.90
16	1270.30	7589.50

OUTPUT FROM AMT-MT FORWARD

FREQ.	OBS-RES	CAL-RES	ANGLE
27000.00	130.00	130.56	37.67
14000.00	165.00	153.81	34.53
7500.00	215.00	186.38	33.20
4500.00	265.00	216.48	33.00
2700.00	305.00	247.08	32.90
1400.00	385.00	291.68	32.00
750.00	505.00	353.06	30.62
450.00	660.00	422.77	29.88
270.00	810.00	507.09	29.61
140.00	1000.00	635.05	29.31
75.00	1300.00	794.71	28.74
45.00	1650.00	973.76	28.47
27.00	2000.00	1208.42	28.89
14.00	2300.00	1585.15	31.09
7.50	2275.00	1946.40	35.09
4.50	2000.00	2146.21	39.16

OUTPUT FROM PLOT

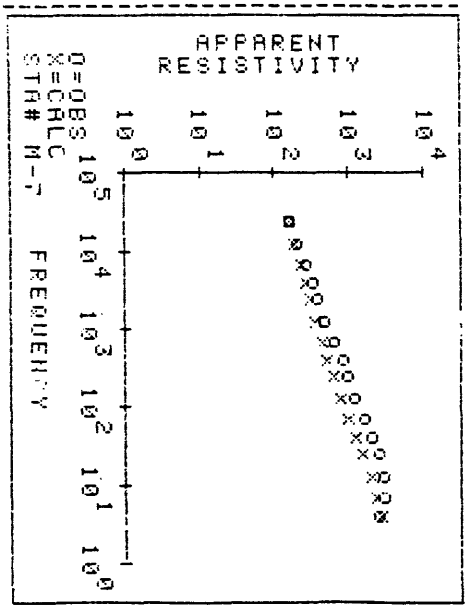

OUTPUT FROM BOSTICK

STA-ID M-8AMP INVER INPUT CURVE

LAYER NO.	RESISTIVITY	DEPTH
1	80.00	19.60
2	222.84	31.18
3	674.99	52.58
4	1141.80	81.39
5	690.81	117.98
6	1002.70	192.43
7	1594.30	311.08
8	2394.50	464.76
9	1646.30	653.61
10	1942.90	1009.10
11	1524.60	1440.00
12	2224.00	1990.00
13	2743.30	2771.30
14	3652.50	4302.80
15	3117.60	6235.40
16	3000.00	8313.80

OUTPUT FROM AMT-MT FORWARD

FREQ.	OBS-RES	CAL-RES	ANGLE
27000.00	80.00	77.90	34.17
14000.00	105.00	99.95	28.77
7500.00	160.00	135.30	26.23
4500.00	230.00	173.03	25.56
2700.00	290.00	218.48	25.28
1400.00	400.00	295.48	24.99
750.00	560.00	397.68	25.23
450.00	750.00	506.02	26.07
270.00	890.00	634.24	27.61
140.00	1100.00	808.38	30.30
75.00	1200.00	957.76	32.66
45.00	1375.00	1069.00	33.77
27.00	1600.00	1192.45	34.11
14.00	2000.00	1397.97	34.25
7.50	2250.00	1638.99	34.85
4.50	2400.00	1848.46	35.79

OUTPUT FROM PLOT

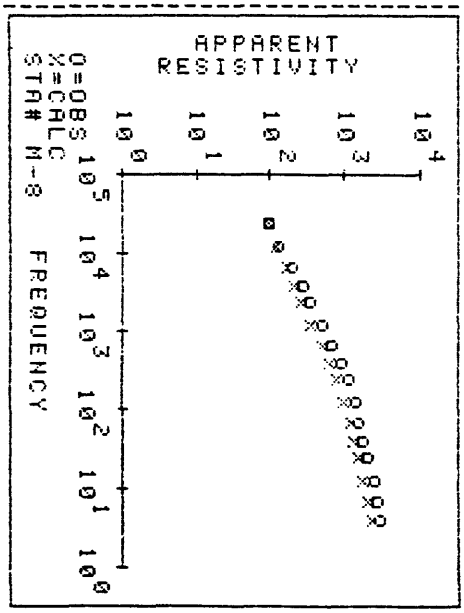

OUTPUT FROM BOSTICK

STA-ID M-9AMP INVER INPUT CURVE

LAYER NO.	RESISTIVITY	DEPTH
1	80.00	19.60
2	80.00	27.21
3	87.72	37.64
4	86.53	48.89
5	107.70	64.99
6	115.80	93.78
7	281.95	146.97
8	488.45	217.99
9	686.14	324.96
10	580.38	513.64
11	628.99	777.69
12	721.42	1086.60
13	1032.10	1549.20
14	884.48	2327.10
15	1128.90	3465.50
16	1316.50	4800.00

OUTPUT FROM AMT-MT FORWARD

FREQ.	OBS-RES	CAL-RES	ANGLE
27000.00	80.00	79.65	44.69
14000.00	80.00	80.05	44.46
7500.00	82.00	80.55	44.18
4500.00	83.00	80.94	43.94
2700.00	88.00	80.51	43.50
1400.00	95.00	79.42	41.50
750.00	125.00	82.73	37.53
450.00	165.00	92.54	33.79
270.00	220.00	110.33	30.81
140.00	285.00	144.43	28.82
75.00	350.00	186.98	28.32
45.00	410.00	229.55	28.48
27.00	500.00	279.15	29.03
14.00	585.00	351.82	30.01
7.50	695.00	430.88	30.93
4.50	800.00	504.86	31.71

OUTPUT FROM PLOT

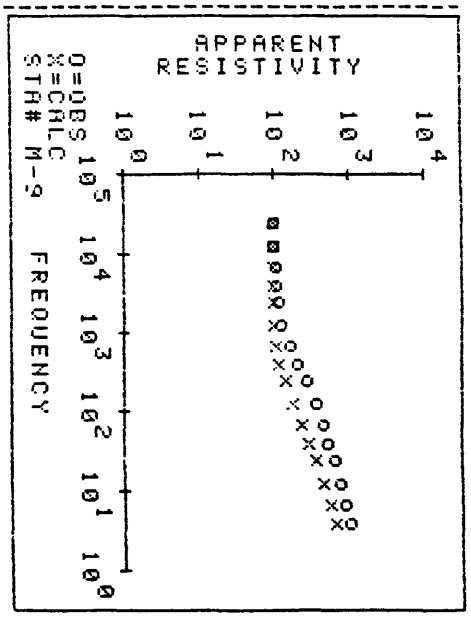

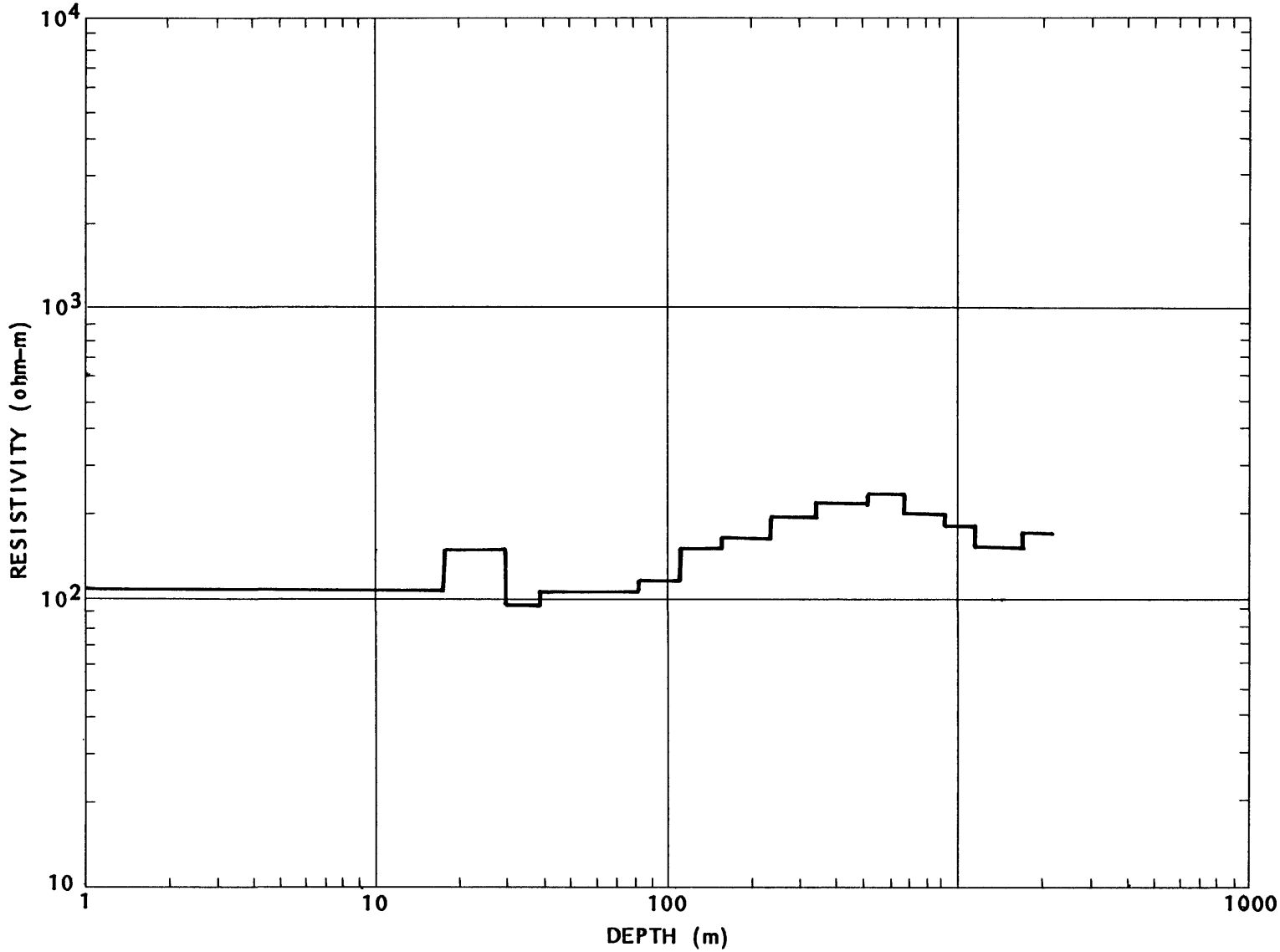

Meshaheed AMT sounding M-1 E/EW

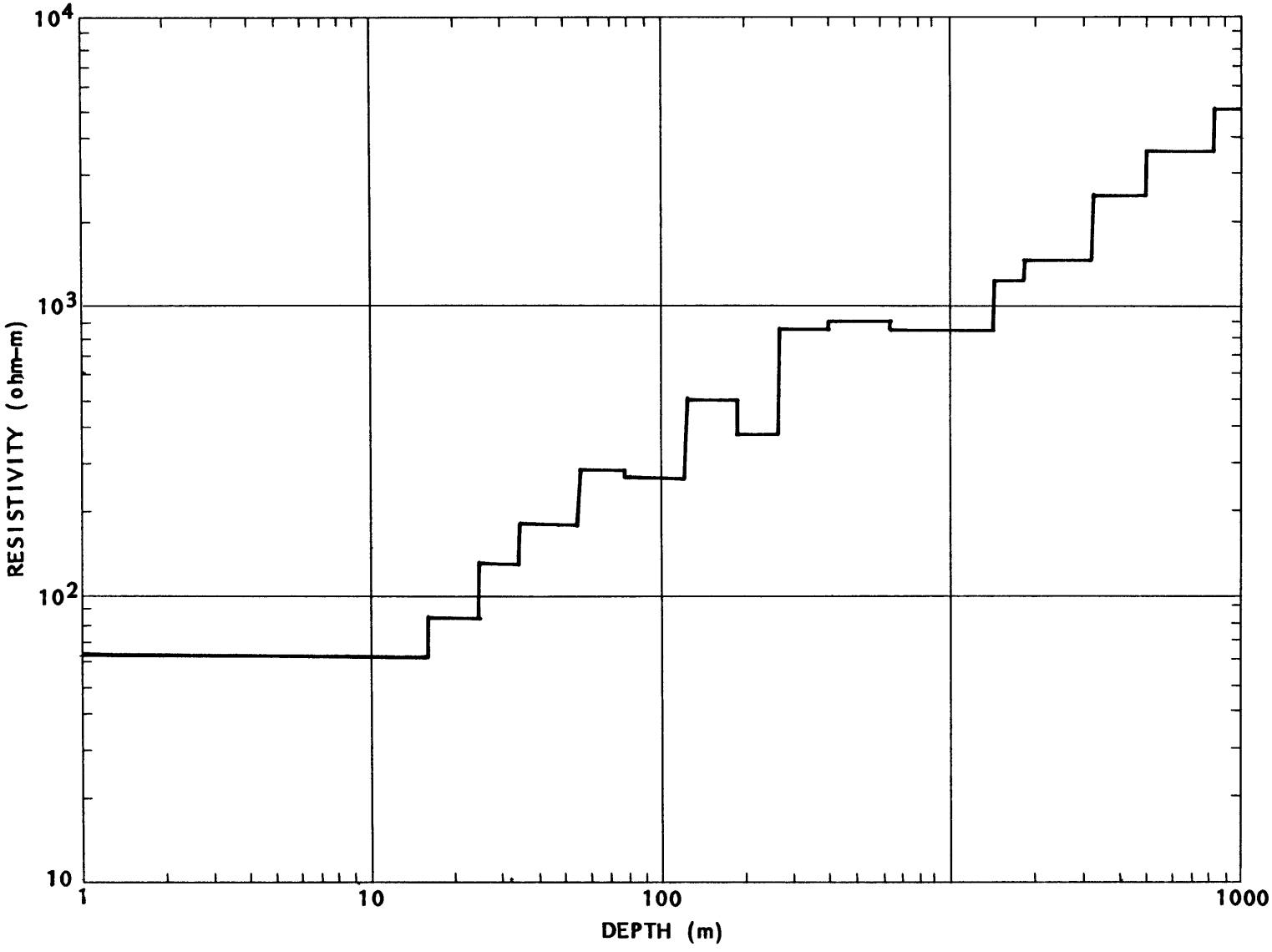

Meshaheed AMT M-4 sounding

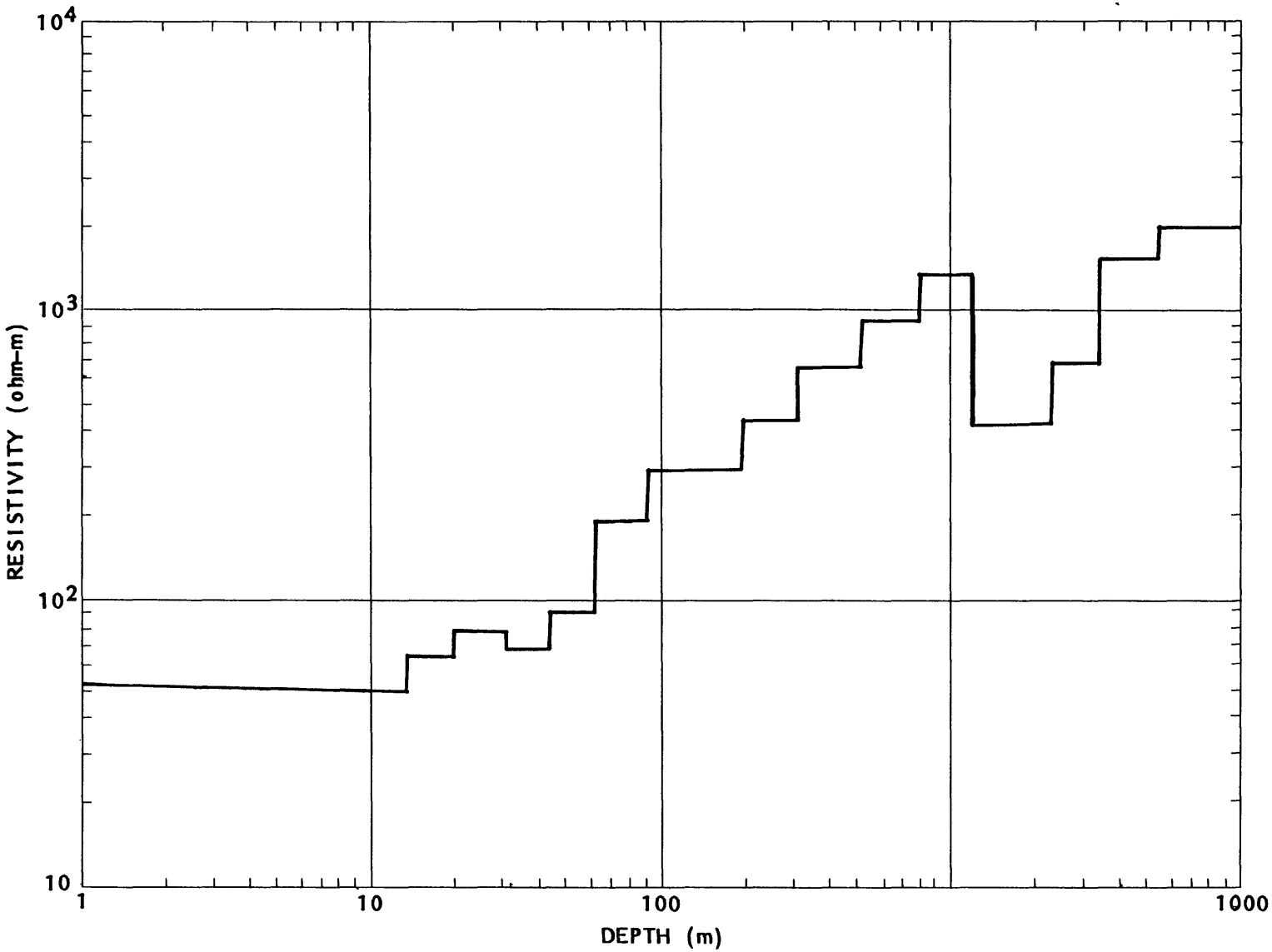

Meshaheed AMT sounding M-6

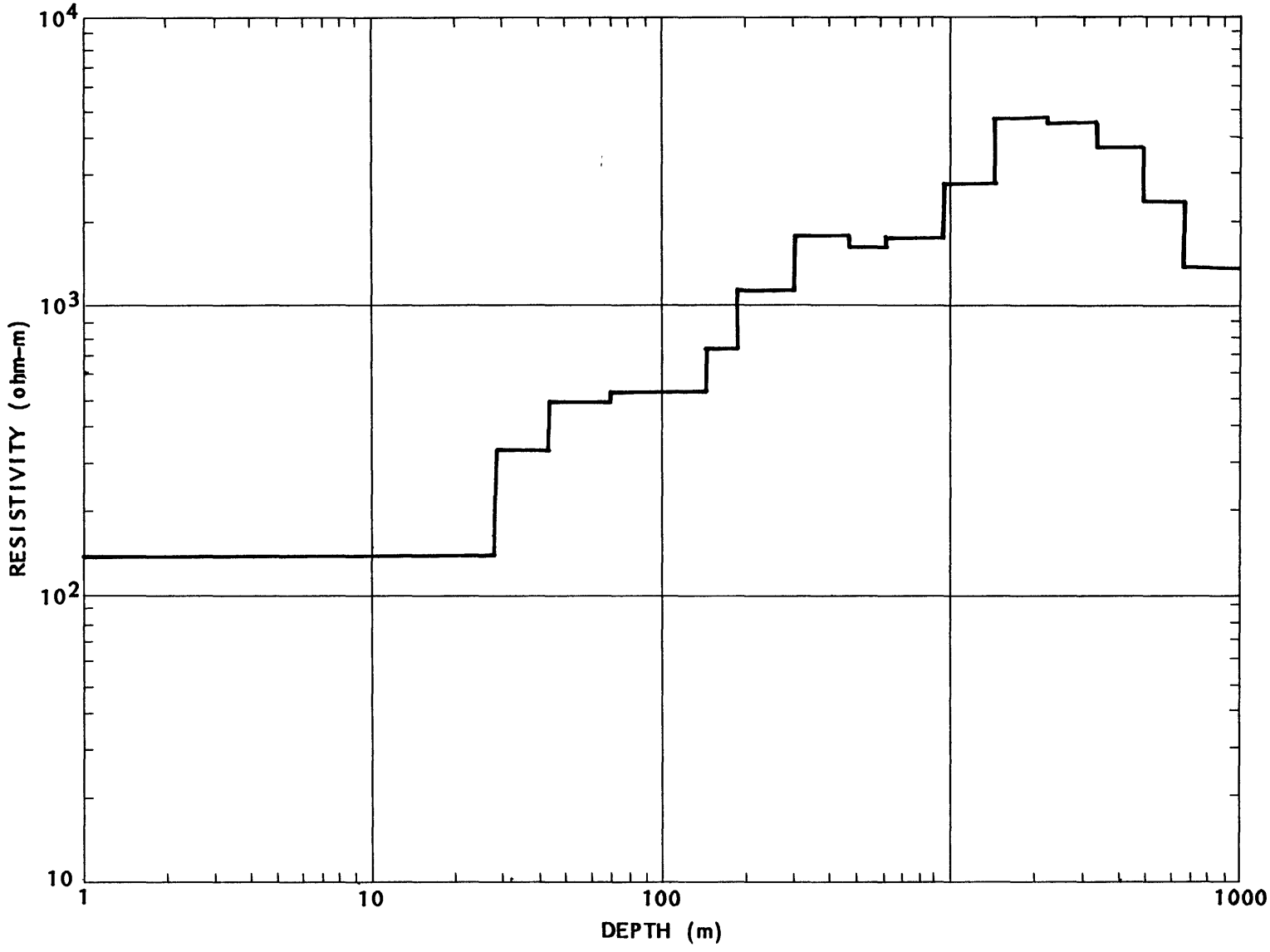

Meshaheed AMT sounding M-7

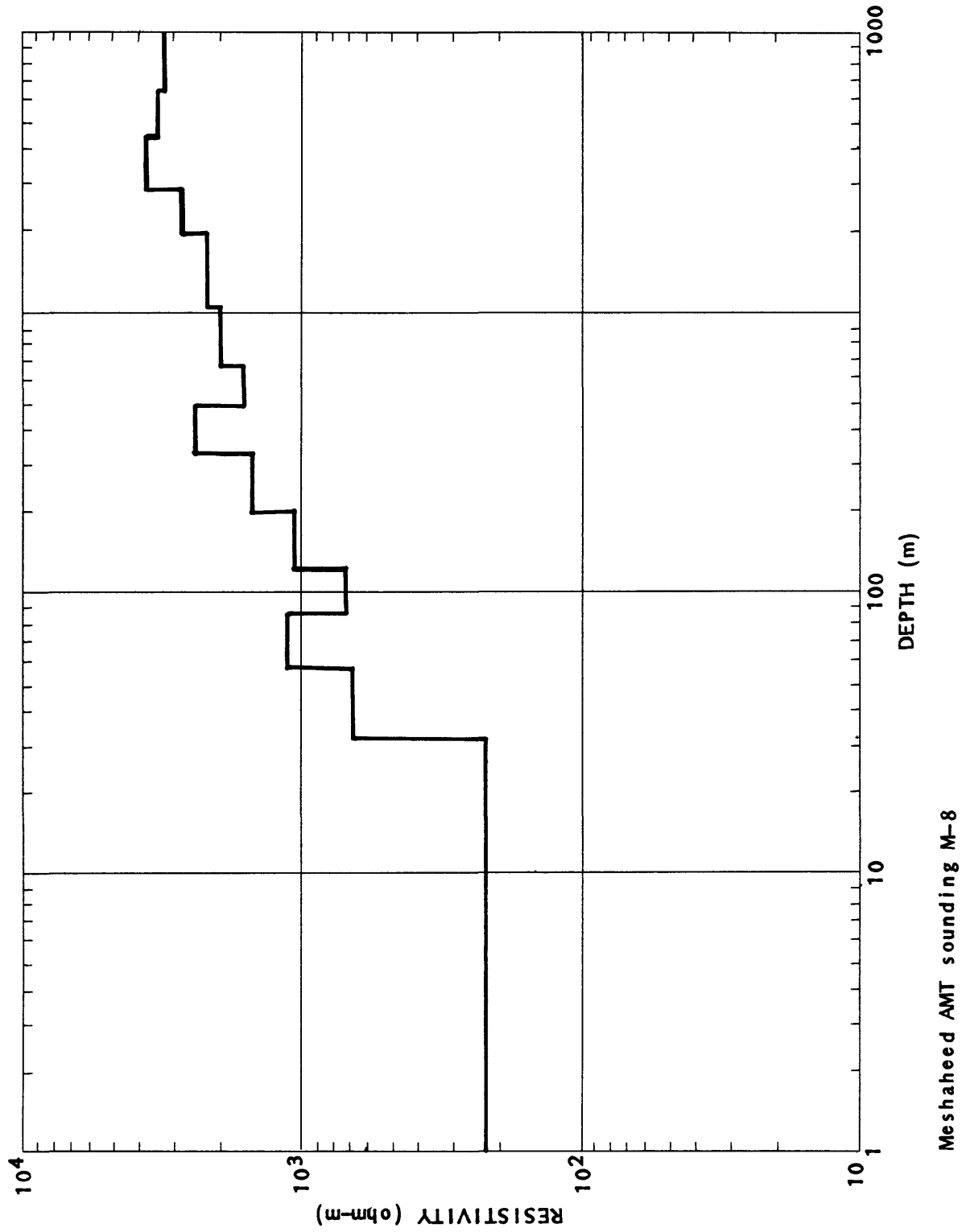
RESISTIVITY (ohm-m)
10^4
10^3
10^2
10^1
1
10
100
1000
DEPTH (m)
Meshaheed AMT sounding M-8

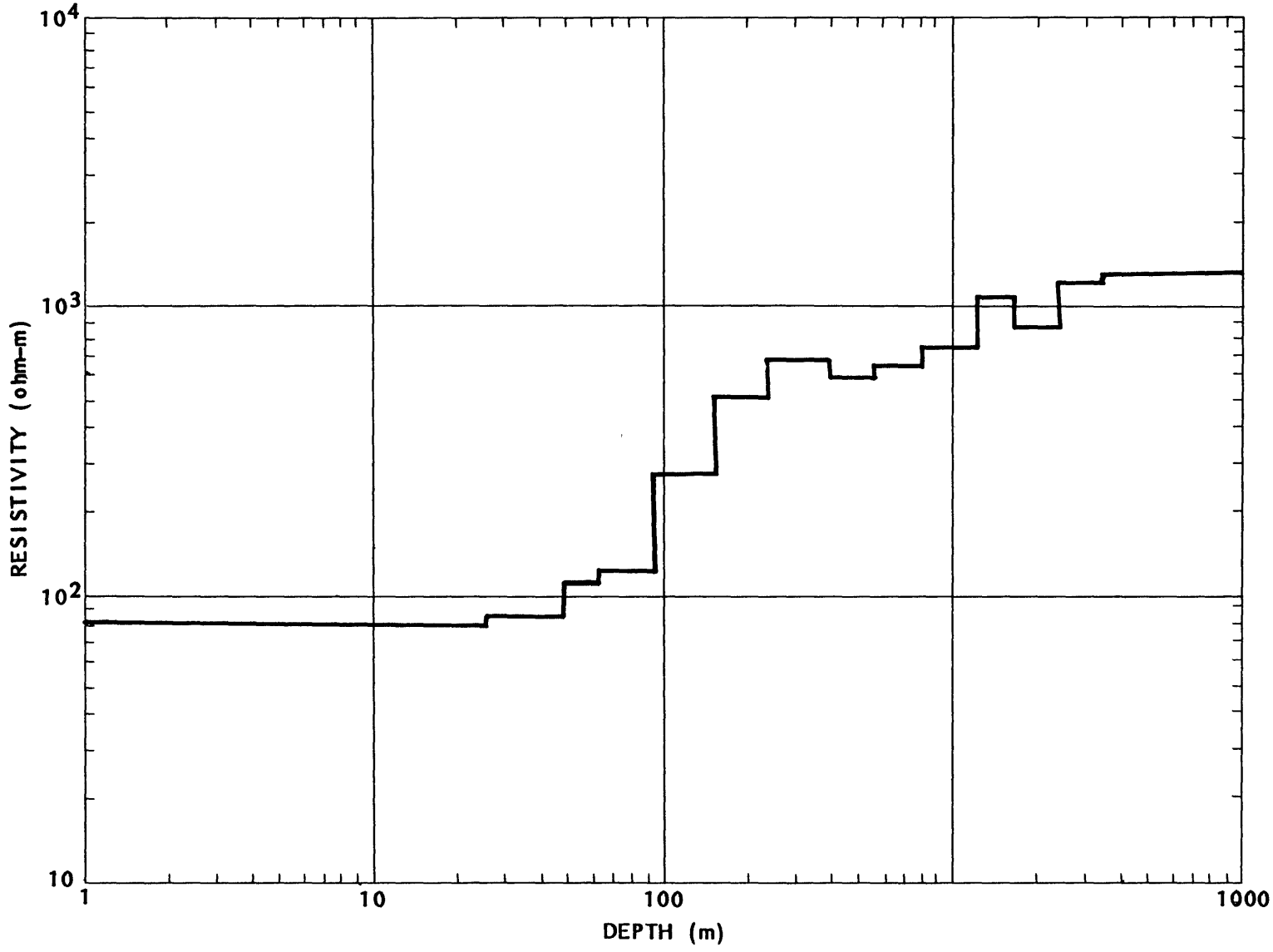

Meshaheed AMT sounding M-9

APPENDIX, PART B

SILSILAH AREA

OUTPUT FROM BOSTICK

STA-ID F-1AMP INVER INPUT CURVE

LAYER NO.	RESISTIVITY	DEPTH
1	85.00	20.20
2	810.31	36.00
3	5152.00	65.73
4	1072.50	98.22
5	859.19	140.29
6	1158.90	223.58
7	1702.50	352.73
8	2327.70	514.74
9	4318.00	774.60
10	8204.80	1343.60
11	8866.80	2199.60
12	30078.00	3477.90
13	28461.00	5366.60
14	46378.00	9427.00
15	39131.00	15274.00
16	67137.00	23082.00

OUTPUT FROM AMT-MT FORWARD

FREQ.	OBS-RES	CAL-RES	ANGLE
27000.00	85.00	93.14	27.87
14000.00	140.00	136.31	23.65
7500.00	250.00	197.90	23.14
4500.00	335.00	259.65	24.14
2700.00	410.00	328.26	25.53
1400.00	540.00	422.69	26.98
750.00	720.00	523.02	27.10
450.00	920.00	628.23	26.22
270.00	1250.00	769.38	24.72
140.00	1950.00	1040.30	22.11
75.00	2800.00	1470.29	19.49
45.00	4200.00	2025.64	17.95
27.00	6000.00	2831.37	17.18
14.00	9600.00	4364.60	17.07
7.50	13500.00	6546.00	17.72
4.50	18500.00	9026.47	18.80

OUTPUT FROM PLOT

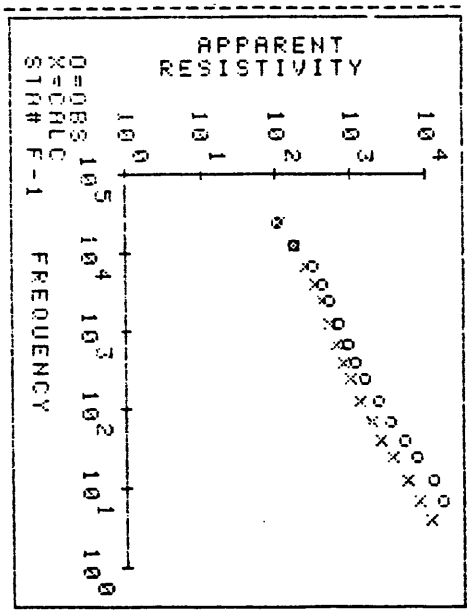

OUTPUT FROM BOSTICK

STA-ID F-2AMP INVER INPUT CURVE

LAYER NO.	RESISTIVITY	DEPTH
1	50.00	15.49
2	85.65	23.17
3	159.37	36.00
4	434.38	54.99
5	4619.90	90.33
6	992.15	155.14
7	1302.10	256.25
8	1152.60	371.81
9	1375.70	536.66
10	3140.30	912.77
11	4225.20	1498.80
12	4800.90	2212.70
13	7761.50	3322.60
14	9572.30	5527.10
15	20468.00	9295.20
16	53696.00	14697.00

OUTPUT FROM AMT-MT FORWARD

FREQ.	OBS-RES	CAL-RES	ANGLE
27000.00	50.00	47.27	39.83
14000.00	58.00	50.46	34.26
7500.00	75.00	61.80	27.88
4500.00	105.00	80.40	23.75
2700.00	170.00	109.74	21.36
1400.00	260.00	165.43	20.77
750.00	380.00	235.01	21.74
450.00	480.00	302.72	22.53
270.00	600.00	385.25	22.85
140.00	900.00	527.35	22.72
75.00	1300.00	717.65	22.48
45.00	1700.00	921.05	22.32
27.00	2300.00	1173.86	21.76
14.00	3300.00	1638.50	19.97
7.50	5000.00	2375.74	18.02
4.50	7500.00	3325.80	17.08

OUTPUT FROM PLOT

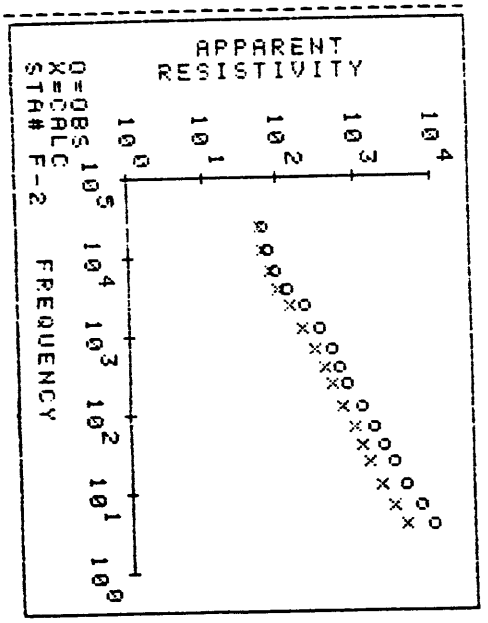

OUTPUT FROM BOSTICK

STA-ID F-5AMP INVER INPUT CURVE

LAYER NO.	RESISTIVITY	DEPTH
1	7.00	5.80
2	11.34	8.61
3	46.62	14.40
4	128.94	22.77
5	133.89	35.33
6	386.44	64.54
7	211.20	105.98
8	297.98	159.20
9	569.77	244.95
10	1152.80	435.63
11	1549.20	743.61
12	3435.50	1175.80
13	1812.70	1739.00
14	2568.00	2886.40
15	6638.70	4918.50
16	9485.10	7589.50

OUTPUT FROM AMT-MT FORWARD

FREQ.	OBS-RES	CAL-RES	ANGLE
27000.00	7.00	6.39	36.96
14000.00	8.00	7.50	29.98
7500.00	12.00	10.03	24.05
4500.00	18.00	13.64	20.81
2700.00	26.00	18.95	19.23
1400.00	45.00	28.53	18.72
750.00	65.00	41.07	18.50
450.00	88.00	55.13	17.89
270.00	125.00	75.32	16.92
140.00	205.00	116.69	16.05
75.00	320.00	178.16	16.39
45.00	480.00	246.21	17.16
27.00	630.00	333.36	17.67
14.00	900.00	492.36	17.66
7.50	1400.00	727.13	17.61
4.50	2000.00	1007.45	18.07

OUTPUT FROM PLOT

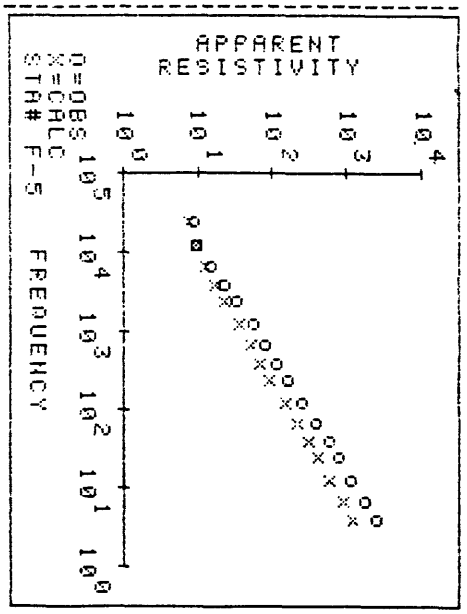

OUTPUT FROM BOSTICK

STA-ID F-6AMP INVER INPUT CURVE

LAYER NO.	RESISTIVITY	DEPTH
1	50.00	15.49
2	65.89	22.36
3	109.85	33.51
4	38.91	40.87
5	111.74	56.71
6	341.38	96.21
7	143.02	137.87
8	62.32	167.14
9	28.01	189.74
10	14.33	215.14
11	25.70	269.40
12	33.81	339.41
13	49.71	449.00
14	79.31	680.34
15	172.95	1084.00
16	387.56	1654.10

OUTPUT FROM AMT-MT FORWARD

FREQ.	OBS-RES	CAL-RES	ANGLE
27000.00	50.00	50.33	41.08
14000.00	54.00	55.99	40.62
7500.00	65.00	58.89	41.54
4500.00	58.00	59.12	41.17
2700.00	67.00	61.09	39.30
1400.00	100.00	70.25	36.92
750.00	110.00	85.14	37.34
450.00	97.00	97.46	40.15
270.00	75.00	104.61	44.70
140.00	50.00	99.53	51.56
75.00	42.00	82.15	56.63
45.00	40.00	66.20	58.49
27.00	42.00	52.80	58.17
14.00	50.00	40.55	54.67
7.50	68.00	34.50	48.00
4.50	95.00	34.18	41.04

OUTPUT FROM PLOT

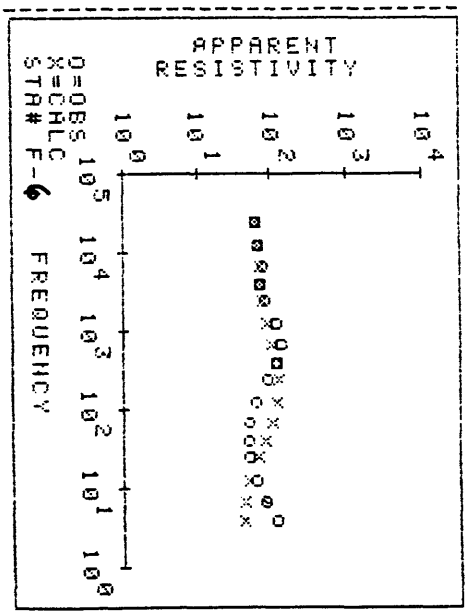

OUTPUT FROM BOSTICK

STA-ID F-7AAMP INVER INPUT CURVE

LAYER NO.	RESISTIVITY	DEPTH
1	90.00	20.79
2	188.07	31.91
3	282.16	49.19
4	468.67	72.00
5	2412.30	114.89
6	449.40	170.76
7	5710.50	305.47
8	1745.80	445.78
9	1352.90	619.68
10	1496.70	937.78
11	2532.40	1452.00
12	2165.20	1997.20
13	4551.60	2918.90
14	3274.40	4409.10
15	4086.10	6572.70
16	5801.20	9295.20

OUTPUT FROM AMT-MT FORWARD

FREQ.	OBS-RES	CAL-RES	ANGLE
27000.00	90.00	88.30	39.08
14000.00	110.00	97.60	34.83
7500.00	140.00	118.21	30.97
4500.00	180.00	142.95	28.79
2700.00	275.00	175.61	26.83
1400.00	315.00	240.21	24.77
750.00	540.00	334.47	24.48
450.00	690.00	431.64	25.56
270.00	800.00	538.64	27.17
140.00	950.00	682.41	29.20
75.00	1220.00	825.43	30.37
45.00	1385.00	962.67	30.75
27.00	1775.00	1127.91	31.04
14.00	2100.00	1375.45	31.47
7.50	2500.00	1651.76	31.72
4.50	3000.00	1924.95	31.87

OUTPUT FROM PLOT

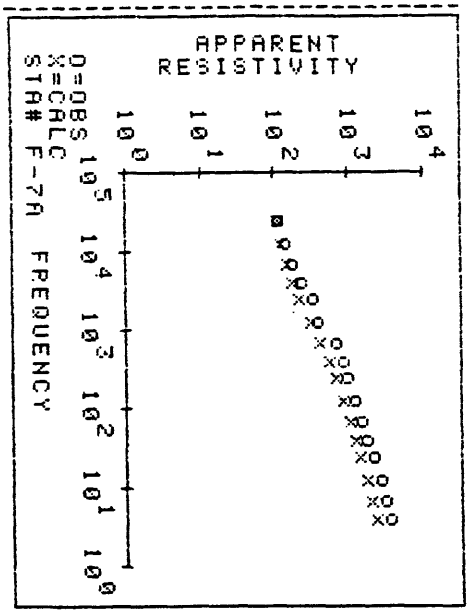

OUTPUT FROM BOSTICK

STA-ID F-8AAMP INVER INPUT CURVE

LAYER NO.	RESISTIVITY	DEPTH
1	125.00	24.50
2	405.86	39.67
3	573.57	63.04
4	836.85	92.95
5	1247.50	138.56
6	2093.10	235.68
7	3496.70	394.36
8	4275.20	593.97
9	3149.70	848.53
10	2920.80	1290.80
11	11764.00	2179.90
12	24420.00	3415.30
13	135140.00	5585.70
14	77651.00	10091.00
15	53608.00	16628.00
16	45874.00	24000.00

OUTPUT FROM AMT-MT FORWARD

FREQ.	OBS-RES	CAL-RES	ANGLE
27000.00	125.00	126.03	36.18
14000.00	170.00	150.23	32.22
7500.00	230.00	186.02	29.23
4500.00	300.00	226.96	27.04
2700.00	400.00	284.82	24.95
1400.00	600.00	401.10	22.97
750.00	900.00	572.52	22.74
450.00	1225.00	748.43	24.04
270.00	1500.00	921.81	25.60
140.00	1800.00	1133.64	25.09
75.00	2750.00	1470.03	21.49
45.00	4050.00	1989.68	19.35
27.00	6500.00	2840.10	16.43
14.00	11000.00	4580.89	16.12
7.50	16000.00	7063.64	17.64
4.50	20000.00	9743.35	19.78

OUTPUT FROM PLOT

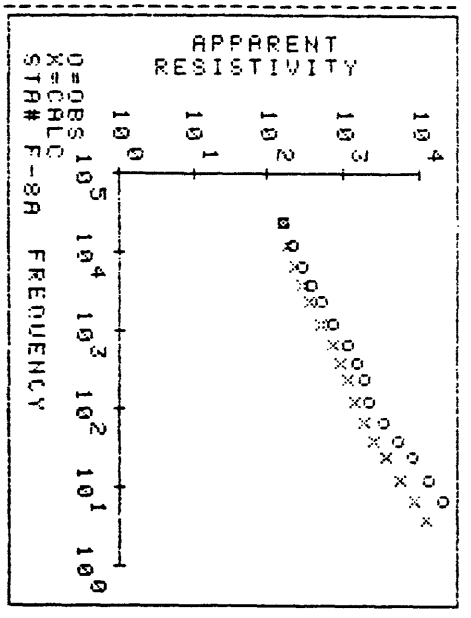

OUTPUT FROM BOSTICK

STA-ID F9AAMP INVER INPUT CURVE

LAYER NO.	RESISTIVITY	DEPTH
1	34.00	12.78
2	74.07	19.72
3	103.87	30.26
4	137.39	43.27
5	171.65	61.97
6	418.70	105.40
7	593.69	173.90
8	1696.50	273.64
9	3826.50	438.18
10	6730.30	804.98
11	3097.40	1314.50
12	10347.00	2075.00
13	6555.00	3106.10
14	31926.00	5692.10
15	24402.00	9659.80
16	50868.00	15179.00

OUTPUT FROM AMT-MT FORWARD

FREQ.	OBS-RES	CAL-RES	ANGLE
27000.00	34.00	34.05	38.70
14000.00	42.00	38.70	35.88
7500.00	53.00	44.81	33.86
4500.00	65.00	50.93	32.19
2700.00	80.00	58.36	30.13
1400.00	120.00	72.14	25.99
750.00	175.00	97.76	21.13
450.00	260.00	134.56	18.07
270.00	400.00	191.34	16.15
140.00	700.00	302.88	15.11
75.00	1000.00	463.18	14.66
45.00	1495.00	654.75	14.21
27.00	2010.00	932.72	13.66
14.00	3500.00	1497.45	13.10
7.50	5400.00	2379.48	13.18
4.50	8000.00	3470.46	13.86

OUTPUT FROM PLOT

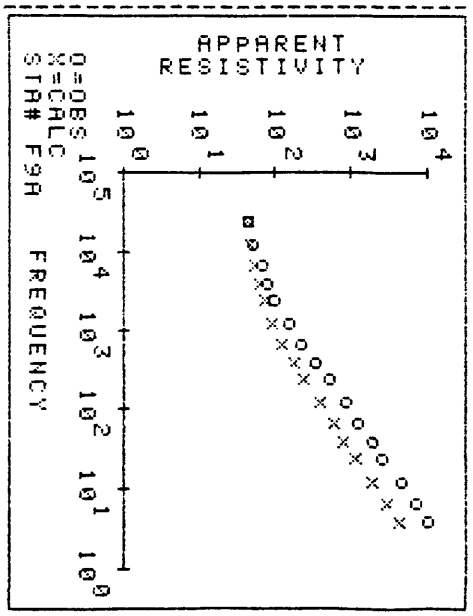

OUTPUT FROM BOSTICK

STA-ID F10AMP INVER INPUT CURVE

LAYER NO.	RESISTIVITY	DEPTH
1	80.00	19.60
2	418.72	33.33
3	1572.50	58.79
4	6140.60	96.00
5	16185.00	157.99
6	340160.00	304.26
7	45421.00	557.71
8	13386.00	865.33
9	11490.00	1296.10
10	8947.70	2041.00
11	7783.60	2997.60
12	12662.00	4259.60
13	14050.00	6000.00
14	18050.00	9377.80
15	28195.00	14697.00
16	40826.00	21466.00

OUTPUT FROM AMT-MT FORWARD

FREQ.	OBS-RES	CAL-RES	ANGLE
27000.00	80.00	74.32	28.77
14000.00	120.00	106.60	18.83
7500.00	200.00	175.34	12.73
4500.00	320.00	274.73	10.26
2700.00	520.00	432.71	9.53
1400.00	1000.00	763.14	10.50
750.00	1800.00	1262.91	13.00
450.00	2600.00	1833.21	16.03
270.00	3500.00	2526.68	19.72
140.00	4500.00	3487.43	24.54
75.00	5200.00	4375.01	28.19
45.00	6300.00	5075.25	30.23
27.00	7500.00	5772.17	31.34
14.00	9500.00	6791.71	31.33
7.50	12500.00	8170.81	30.36
4.50	16000.00	9781.85	29.63

OUTPUT FROM PLOT

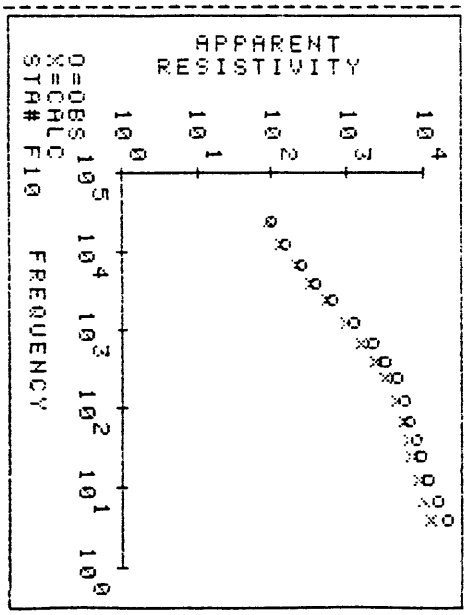

OUTPUT FROM BOSTICK

STA-ID F-11AMP INVER INPUT CURVE

LAYER NO.	RESISTIVITY	DEPTH
1	95.00	21.35
2	9733.00	40.82
3	1176.90	68.94
4	1758.20	105.98
5	1440.60	156.46
6	2403.00	253.49
7	1971.50	407.29
8	1779.50	562.85
9	2366.30	789.94
10	7850.90	1360.70
11	90825.00	2494.20
12	86576.00	4051.70
13	57461.00	6387.50
14	49605.00	10970.00
15	75769.00	18356.00
16	104180.00	27885.00

OUTPUT FROM AMT-MT FORWARD

FREQ.	OBS-RES	CAL-RES	ANGLE
27000.00	95.00	105.72	28.40
14000.00	180.00	149.66	23.90
7500.00	275.00	215.08	22.08
4500.00	390.00	289.88	21.80
2700.00	510.00	388.18	22.45
1400.00	750.00	549.25	24.62
750.00	960.00	708.72	27.78
450.00	1100.00	801.19	29.38
270.00	1300.00	984.86	28.01
140.00	2000.00	1123.35	22.89
75.00	3600.00	1625.97	18.30
45.00	5700.00	2320.86	16.02
27.00	8500.00	3358.78	14.92
14.00	13000.00	5403.84	14.70
7.50	19500.00	8411.41	15.45
4.50	27000.00	11911.93	16.69

OUTPUT FROM PLOT

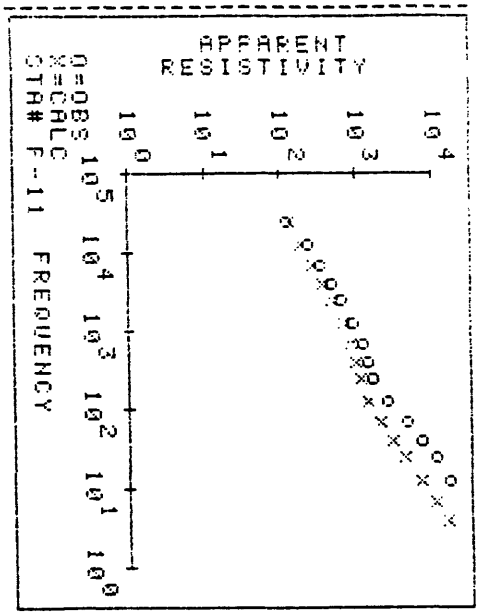

OUTPUT FROM BOSTICK

STA-ID F12AMP INVER INPUT CURVE

LAYER NO.	RESISTIVITY	DEPTH
1	35.00	12.96
2	117.93	21.08
3	365.26	36.00
4	311.79	53.67
5	3068.70	87.64
6	2690.30	161.00
7	5080.00	288.00
8	3042.70	442.54
9	3103.50	664.53
10	3558.50	1097.00
11	3753.60	1713.90
12	5910.20	2517.10
13	10576.00	3794.70
14	9953.70	6160.70
15	17235.00	10011.00
16	30152.00	15179.00

OUTPUT FROM AMT-MT FORWARD

FREQ.	OBS-RES	CAL-RES	ANGLE
27000.00	35.00	34.08	33.86
14000.00	48.00	41.77	27.24
7500.00	75.00	57.26	21.03
4500.00	100.00	80.49	17.15
2700.00	160.00	117.94	14.87
1400.00	280.00	195.35	14.12
750.00	480.00	309.96	15.10
450.00	680.00	440.56	16.72
270.00	920.00	604.95	18.83
140.00	1300.00	857.97	21.39
75.00	1700.00	1151.35	22.95
45.00	2200.00	1449.59	23.68
27.00	3000.00	1813.14	23.97
14.00	4100.00	2430.91	23.57
7.50	5800.00	3301.01	22.87
4.50	8000.00	4319.63	22.67

OUTPUT FROM PLOT

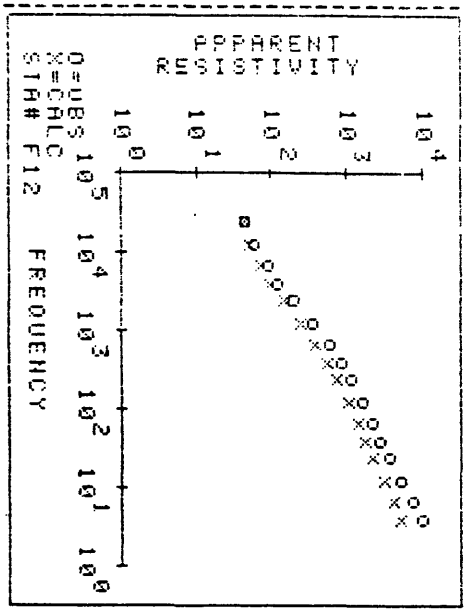

OUTPUT FROM BOSTICK

STA-ID F13AMP INVER INPUT CURVE

LAYER NO.	RESISTIVITY	DEPTH
1	25.00	10.95
2	62.77	17.21
3	93.92	26.94
4	220.29	40.87
5	200.66	60.00
6	785.50	107.57
7	5671.50	197.18
8	2631.10	312.92
9	1551.90	469.89
10	2407.30	799.21
11	2532.80	1281.20
12	2880.40	1859.00
13	6107.40	2814.20
14	5988.40	4614.30
15	14655.00	7776.90
16	17492.00	11758.00

OUTPUT FROM AMT-MT FORWARD

FREQ.	OBS-RES	CAL-RES	ANGLE
27000.00	25.00	34.69	37.54
14000.00	32.00	28.54	33.65
7500.00	42.00	33.66	30.23
4500.00	58.00	39.82	26.35
2700.00	75.00	50.94	21.98
1400.00	125.00	77.55	17.83
750.00	225.00	120.85	16.13
450.00	340.00	173.87	16.05
270.00	460.00	246.48	16.85
140.00	690.00	371.08	18.56
75.00	950.00	535.58	20.13
45.00	1200.00	682.18	21.02
27.00	1650.00	877.03	21.25
14.00	2300.00	1231.45	20.73
7.50	3500.00	1751.74	20.31
4.50	4800.00	2362.49	20.56

OUTPUT FROM PLOT

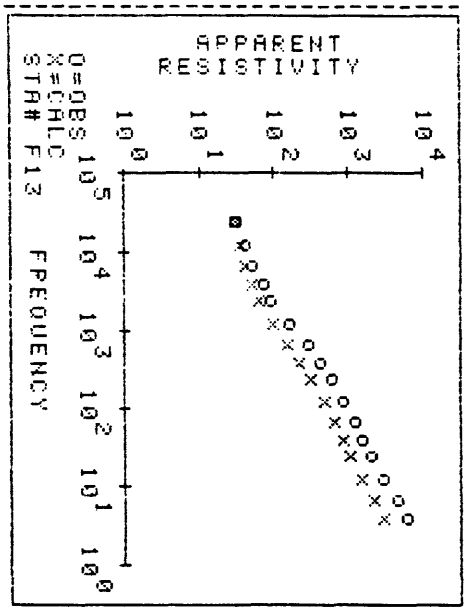

OUTPUT FROM BOSTICK

STA-ID F14AMP INVER INPUT CURVE

LAYER NO.	RESISTIVITY	DEPTH
1	47.00	15.02
2	67.61	21.94
3	171.37	34.78
4	326.04	52.31
5	849.14	81.98
6	1115.70	144.32
7	828.31	231.45
8	858.33	332.99
9	1030.00	477.49
10	1130.40	745.27
11	1205.20	1115.40
12	1334.60	1541.40
13	1489.10	2124.10
14	2334.70	3333.00
15	15725.00	5878.80
16	10851.00	8939.80

OUTPUT FROM AMT-MT FORWARD

FREQ.	OBS-RES	CAL-RES	ANGLE
27000.00	47.00	44.20	39.72
14000.00	52.00	47.94	34.66
7500.00	70.00	57.90	29.06
4500.00	95.00	73.69	25.28
2700.00	140.00	98.24	23.05
1400.00	225.00	144.05	22.40
750.00	310.00	202.50	23.35
450.00	385.00	260.72	24.70
270.00	475.00	327.63	26.28
140.00	600.00	424.71	28.43
75.00	720.00	524.96	30.58
45.00	825.00	598.62	32.28
27.00	940.00	654.06	32.77
14.00	1200.00	744.80	30.41
7.50	2000.00	931.23	26.69
4.50	2775.00	1197.26	24.32

OUTPUT FROM PLOT

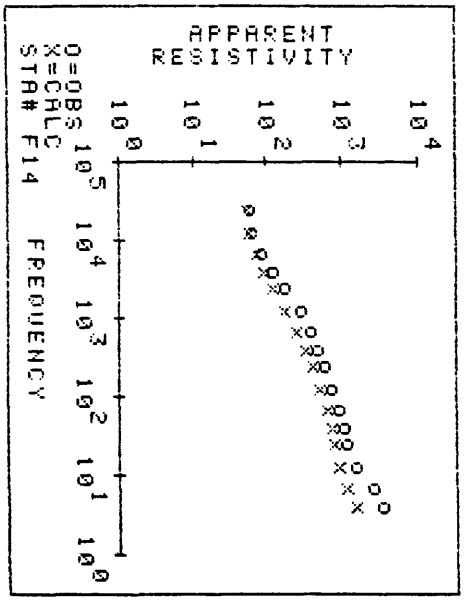

OUTPUT FROM BOSTICK

STA-ID F15AMP INVER INPUT CURVE

LAYER NO.	RESISTIVITY	DEPTH
1	384.99	42.99
2	482.36	61.61
3	954.45	93.88
4	1772.50	137.87
5	1891.40	199.00
6	2994.10	326.28
7	3283.20	509.12
8	6234.80	758.95
9	7138.70	1117.10
10	6307.60	1747.80
11	4573.80	2494.20
12	6122.30	3415.30
13	4761.20	4490.00
14	5377.00	6454.20
15	6193.60	9201.70
16	9762.80	12812.00

OUTPUT FROM AMT-MT FORWARD

FREQ.	OBS-RES	CAL-RES	ANGLE
27000.00	385.00	368.47	41.26
14000.00	410.00	394.71	37.89
7500.00	510.00	448.56	34.71
4500.00	660.00	517.79	32.50
2700.00	825.00	610.63	30.81
1400.00	1150.00	767.98	28.98
750.00	1500.00	983.26	27.35
450.00	2000.00	1239.08	26.52
270.00	2600.00	1578.66	26.71
140.00	3300.00	2107.04	28.37
75.00	3600.00	2653.50	30.76
45.00	4050.00	3091.92	32.99
27.00	4200.00	3479.26	35.23
14.00	4500.00	3840.64	37.57
7.50	4900.00	4082.64	38.47
4.50	5700.00	4318.09	38.27

OUTPUT FROM PLOT

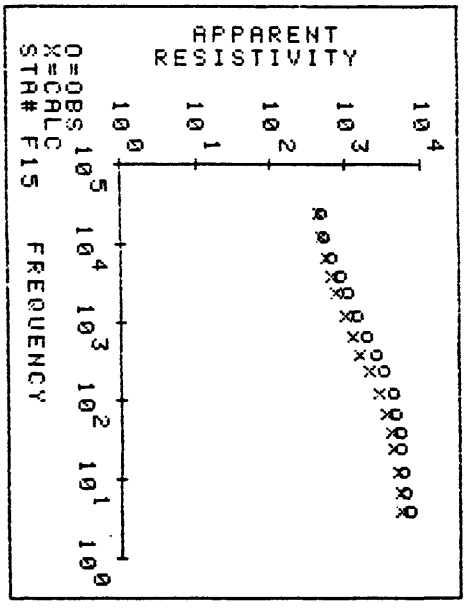

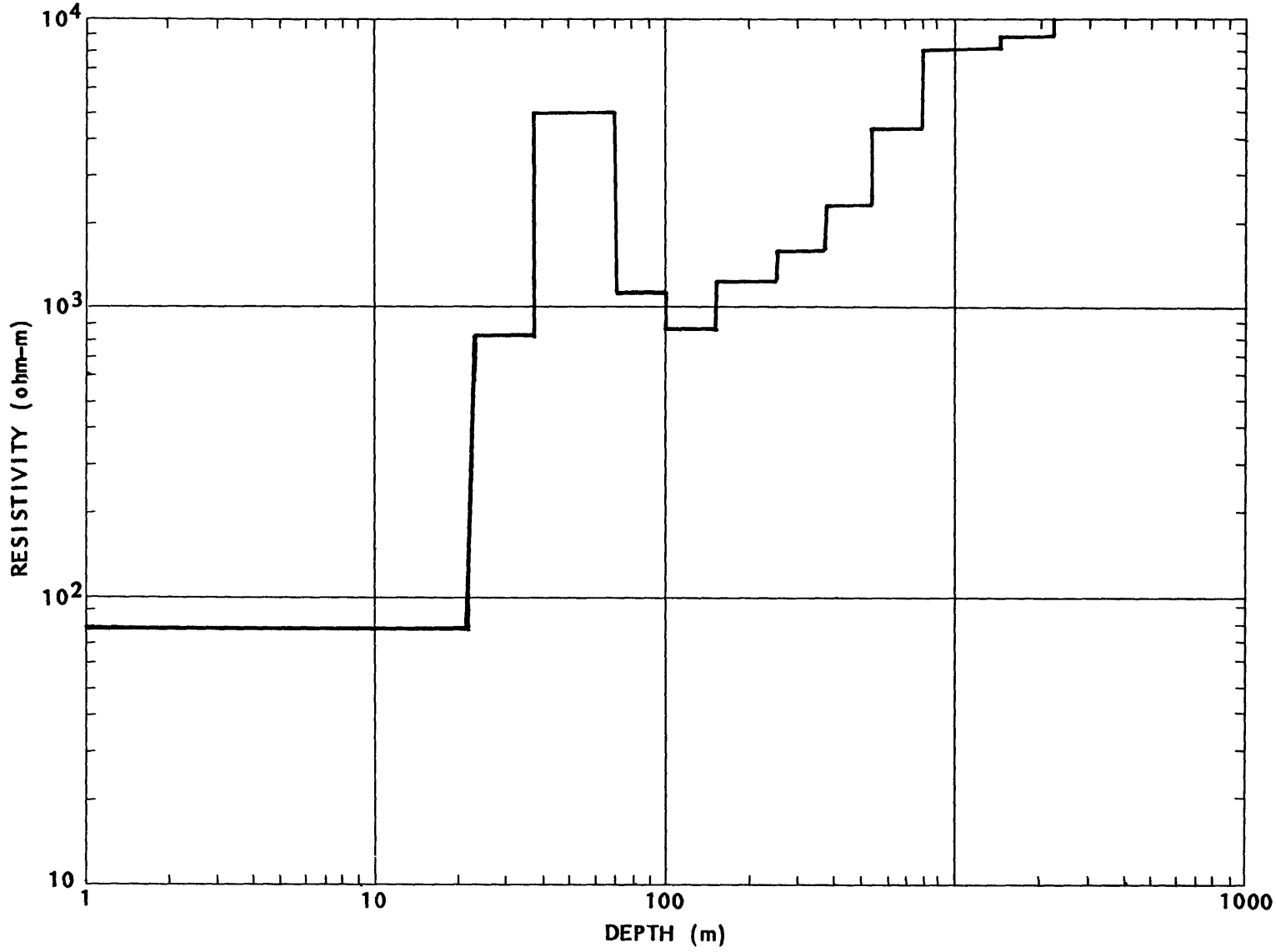

Silsilah AMT sounding F-1 interpreted geoelectric section

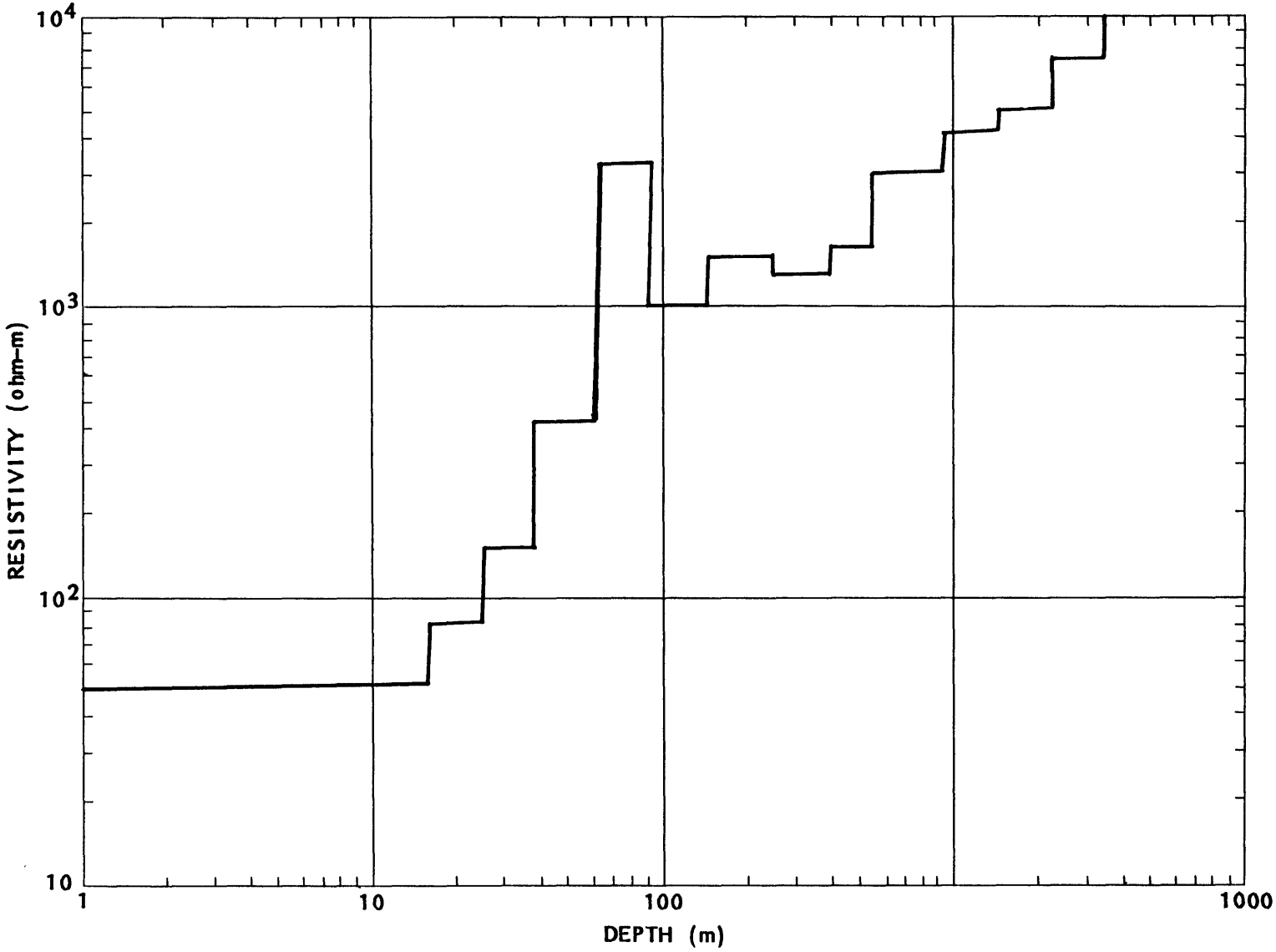

Silsilah AMT sounding F-2

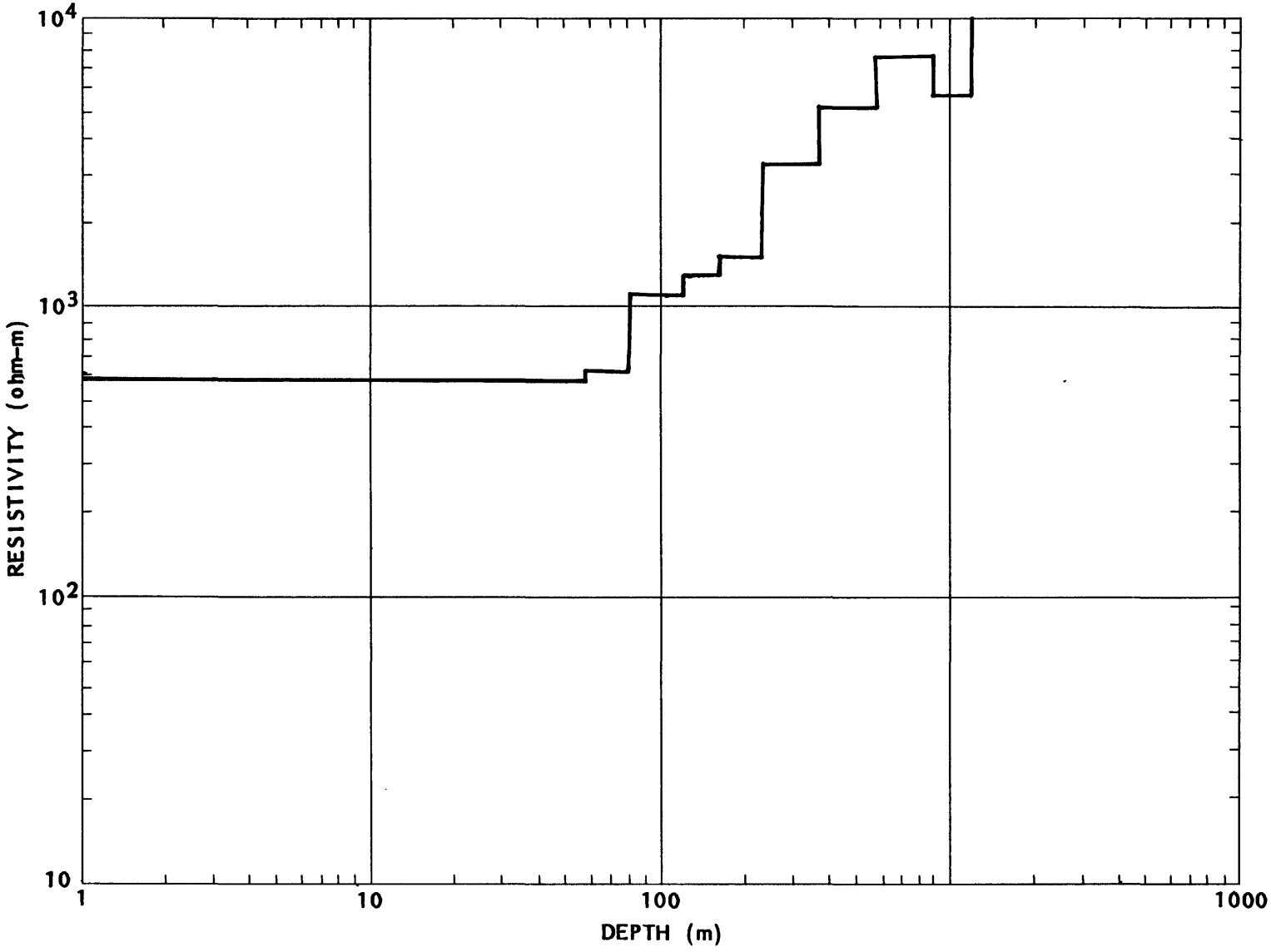

Silsilah AMT sounding F-3

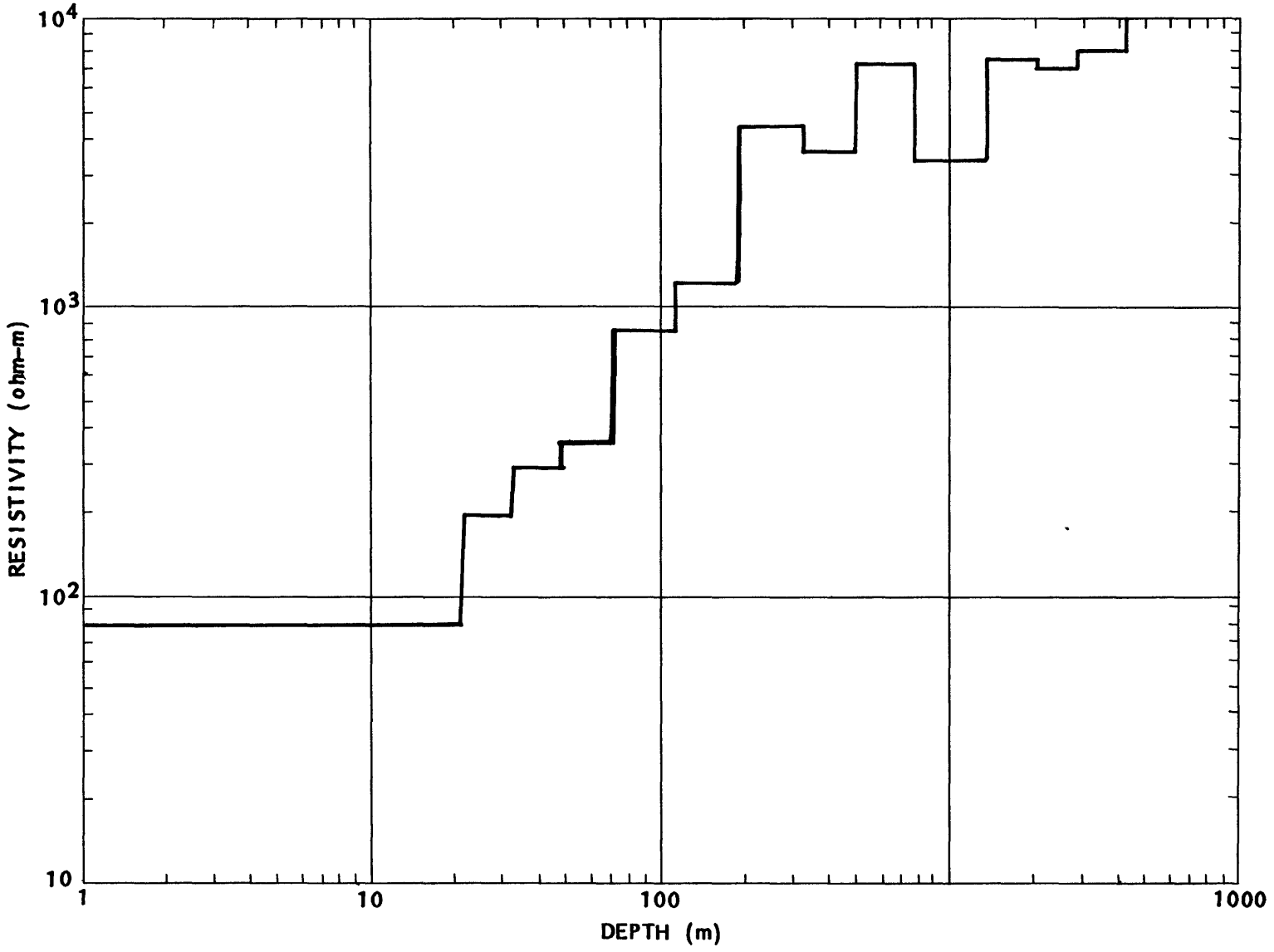

Silsilah AMT sounding F-4

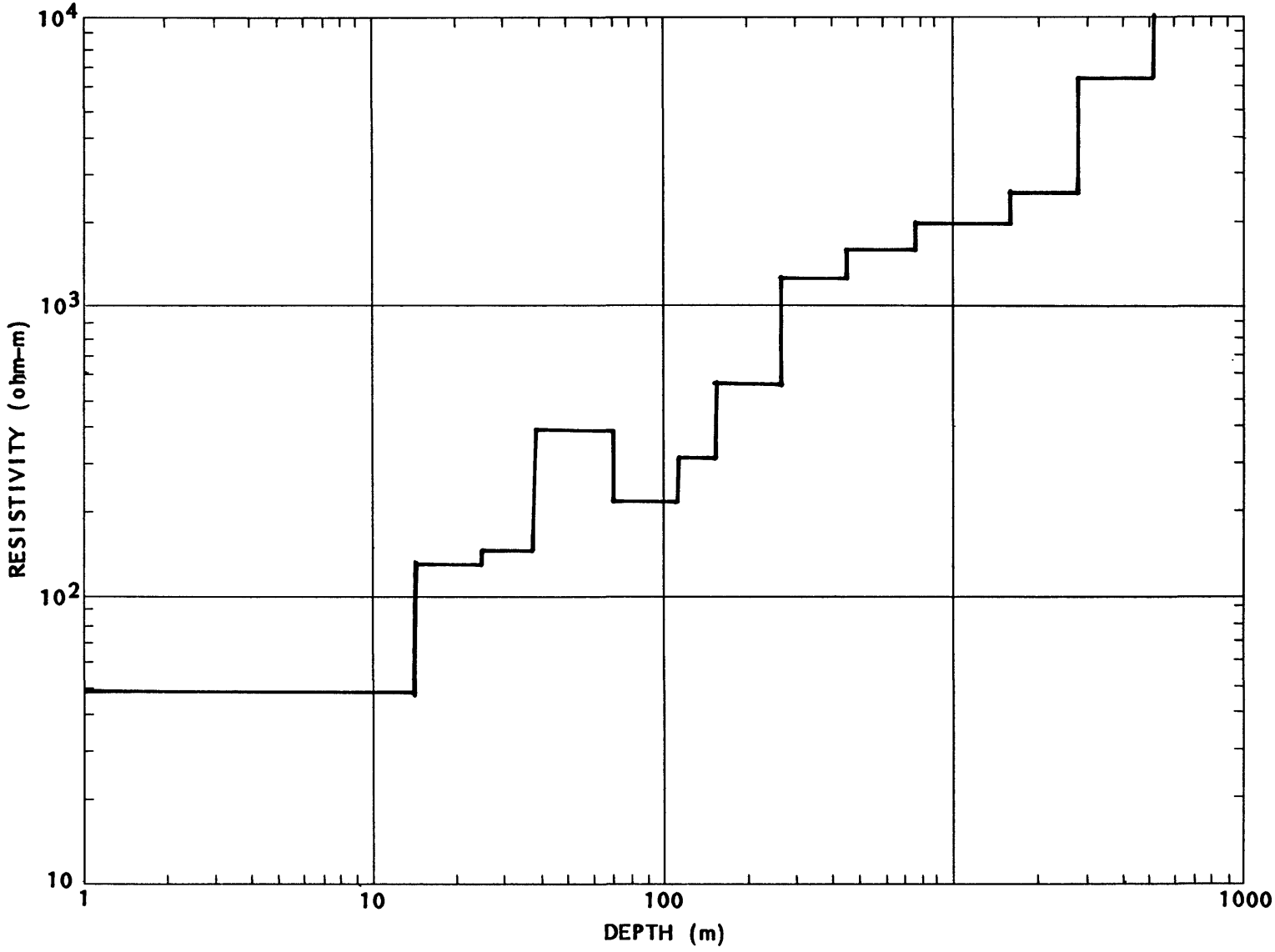

Silsilah AMT sounding F-5

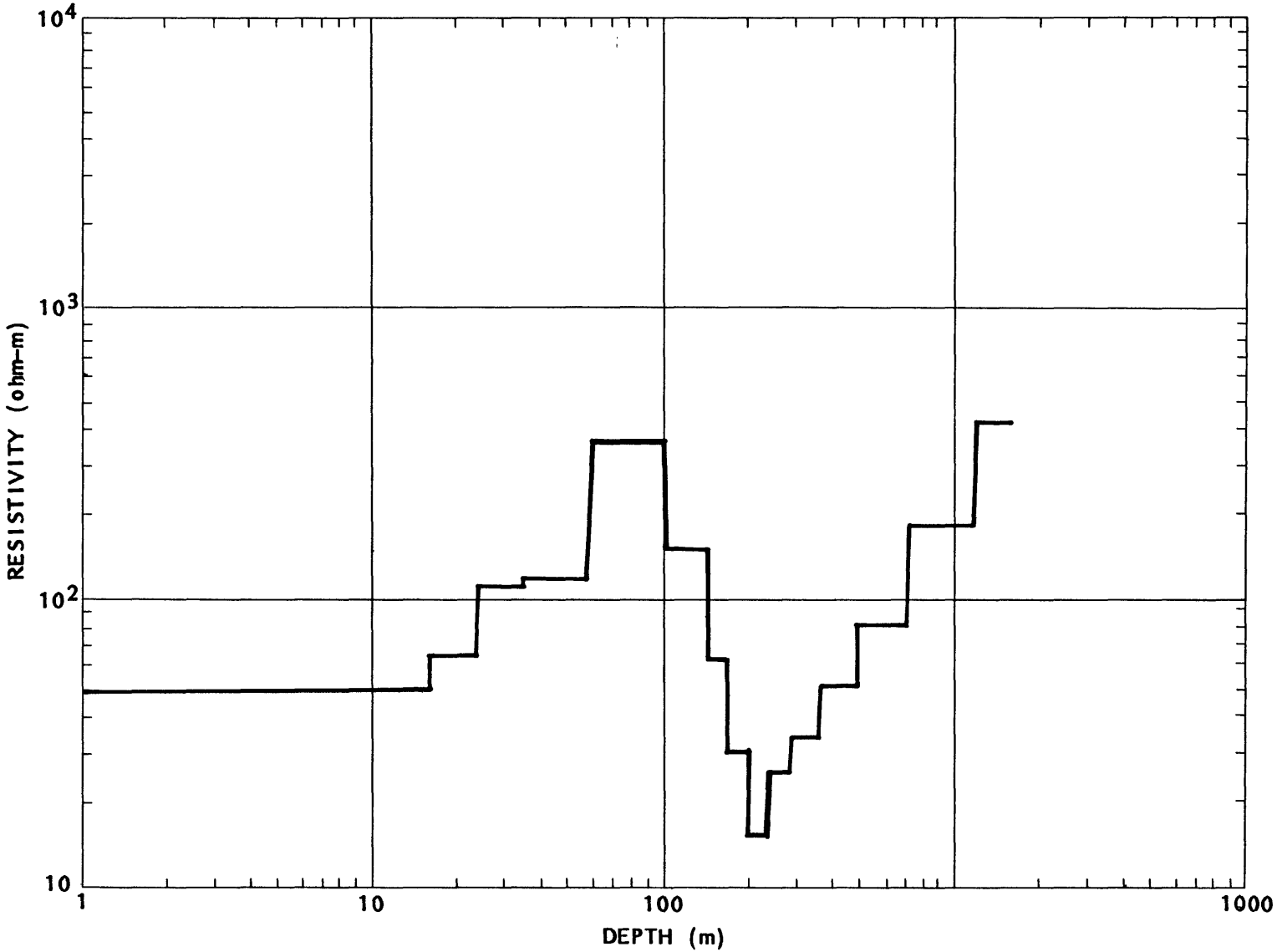

Silsilah AMT sounding F-6

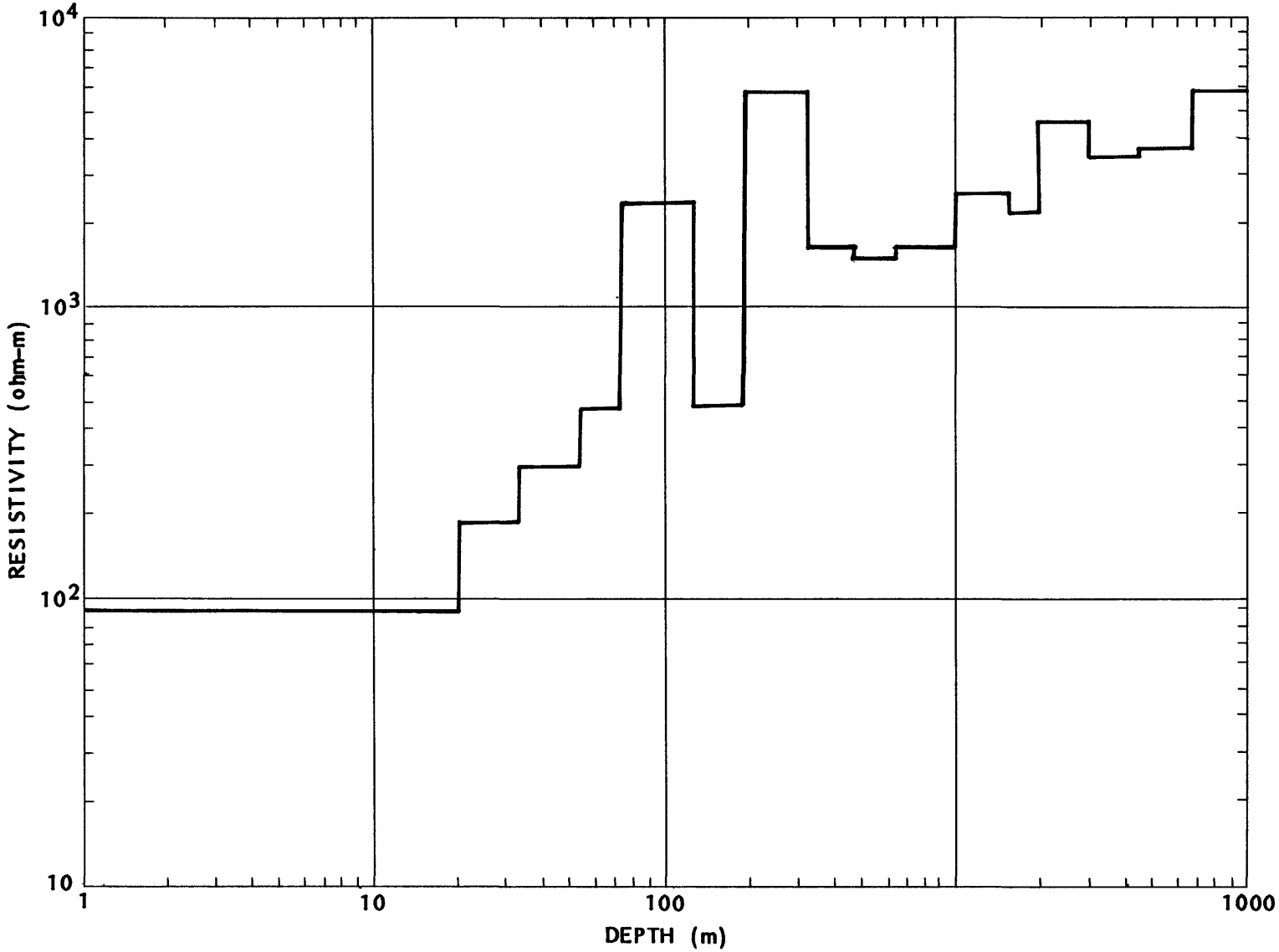

Silsilah AMT sounding F-7

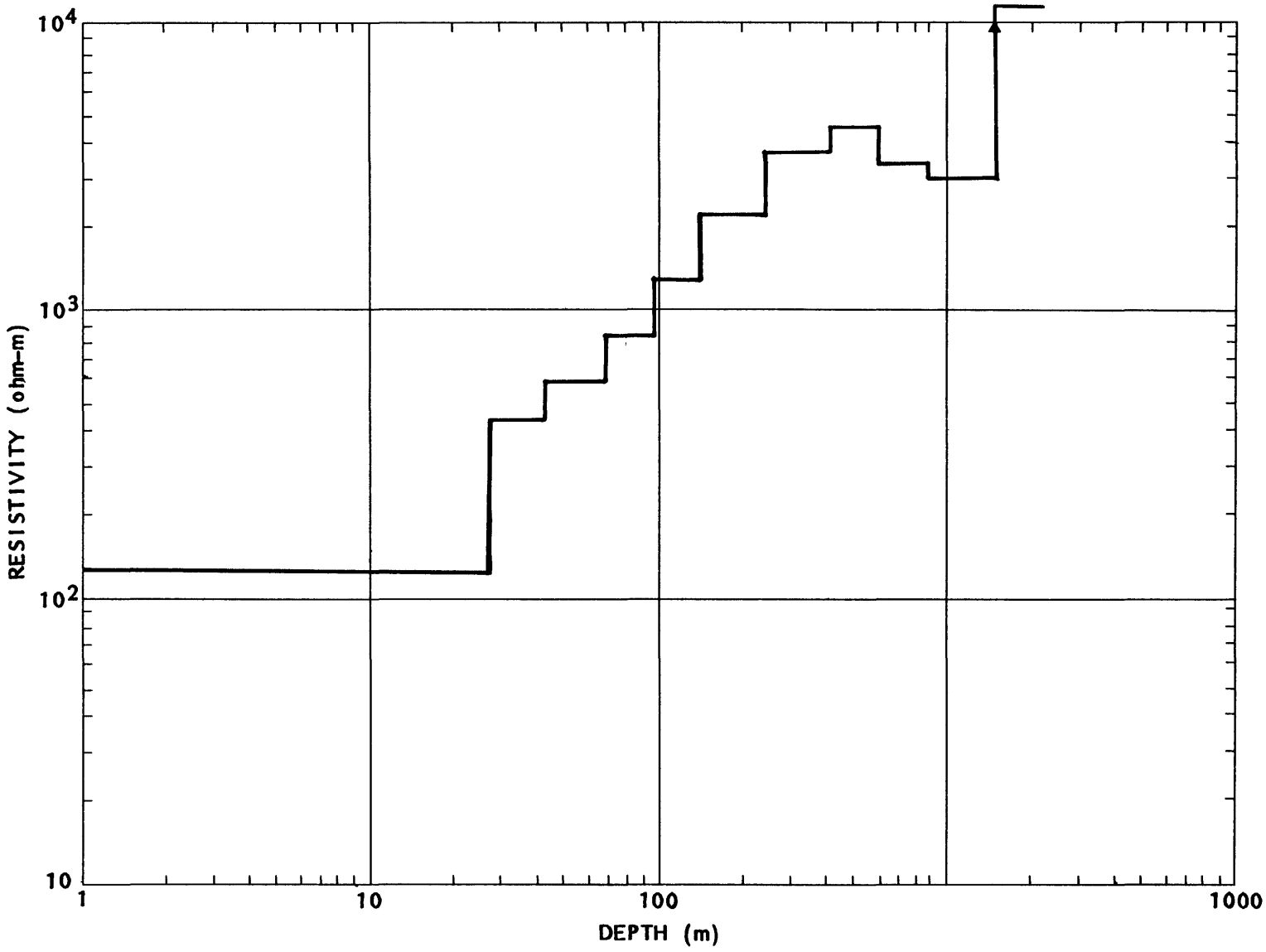

Silsilah AMT sounding F-8

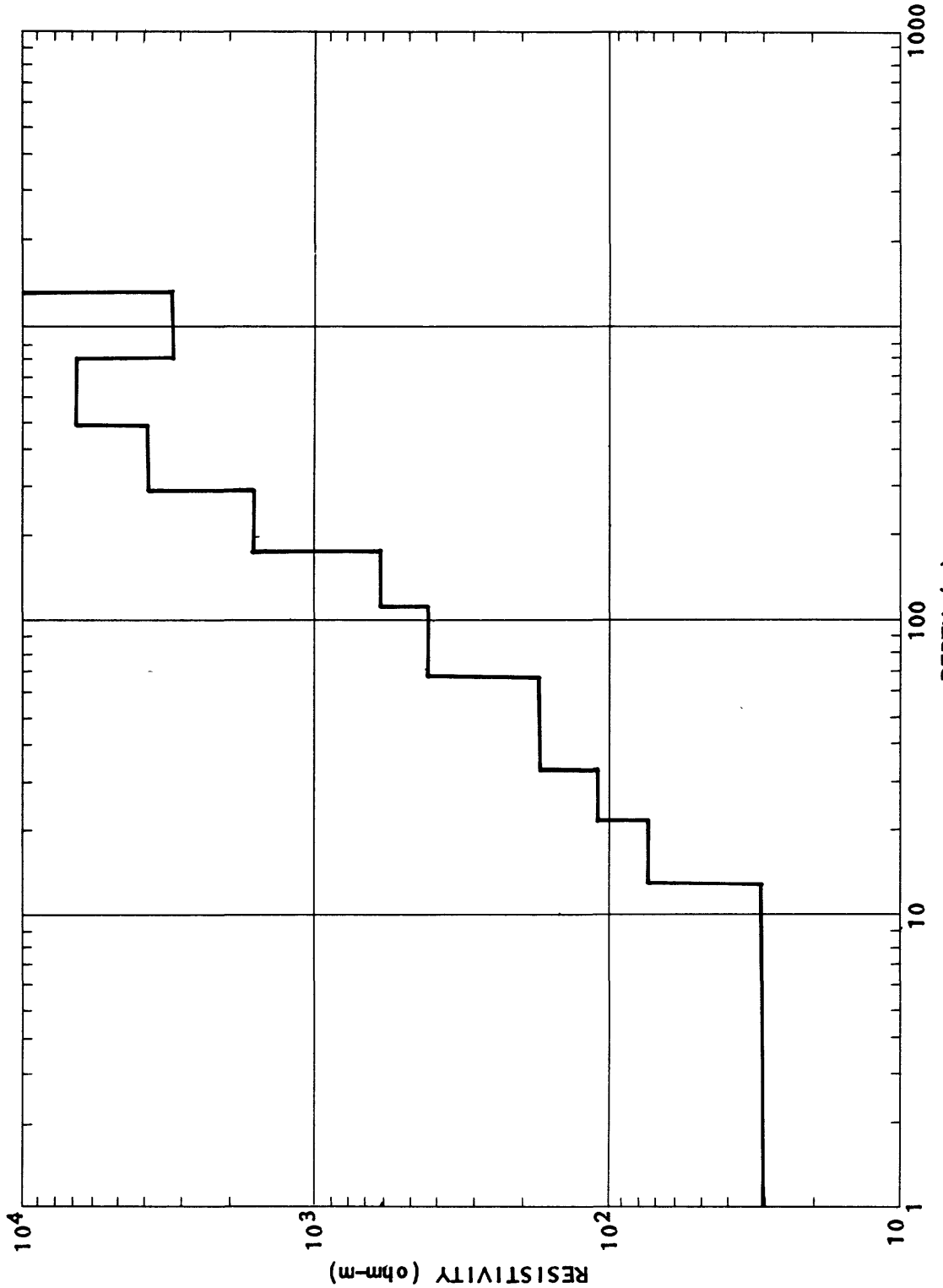

Silsilah ring complex AMT sounding F-9

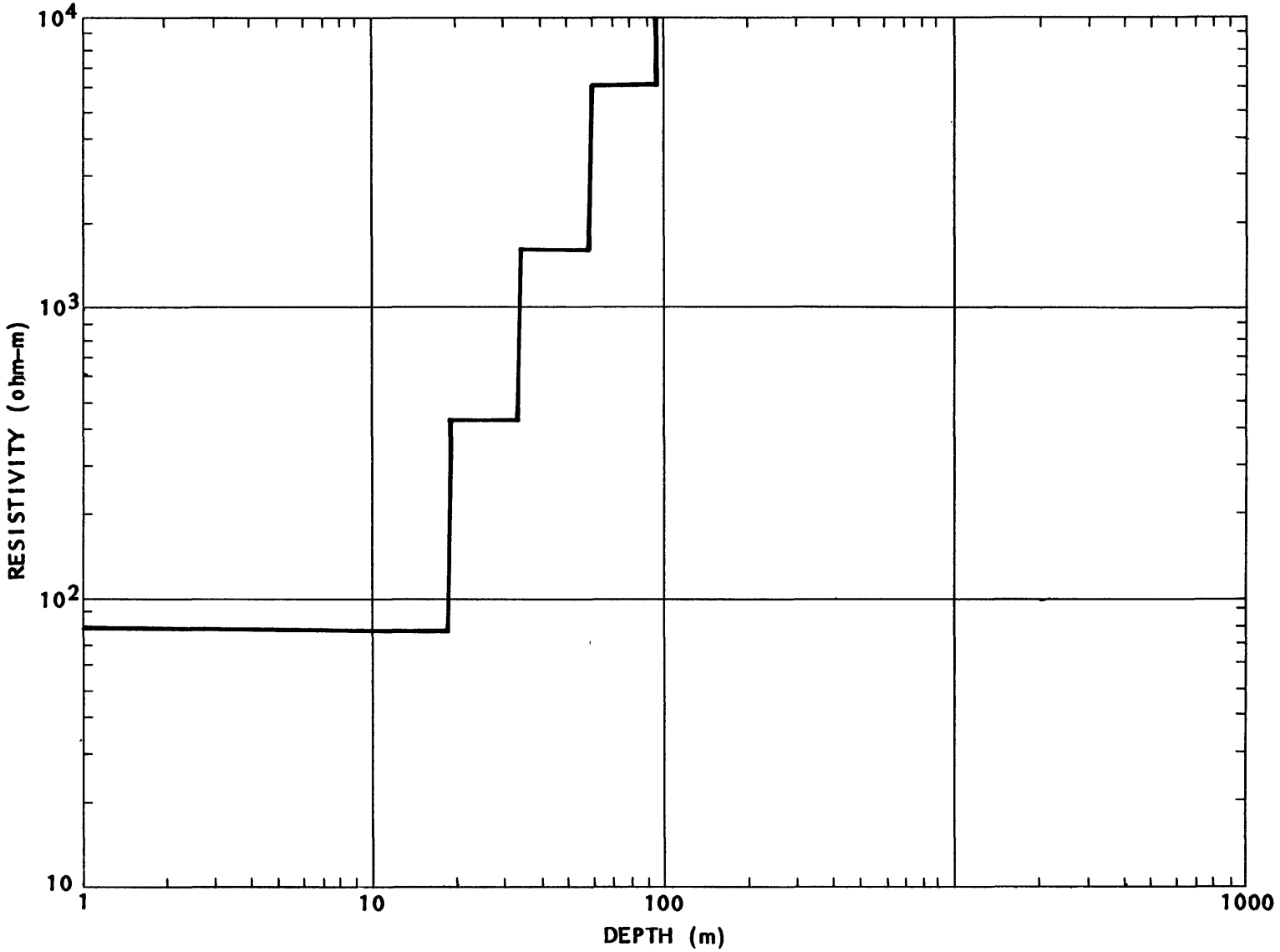

AMT sounding (F-10) between Siisilah tin greisen outcrops

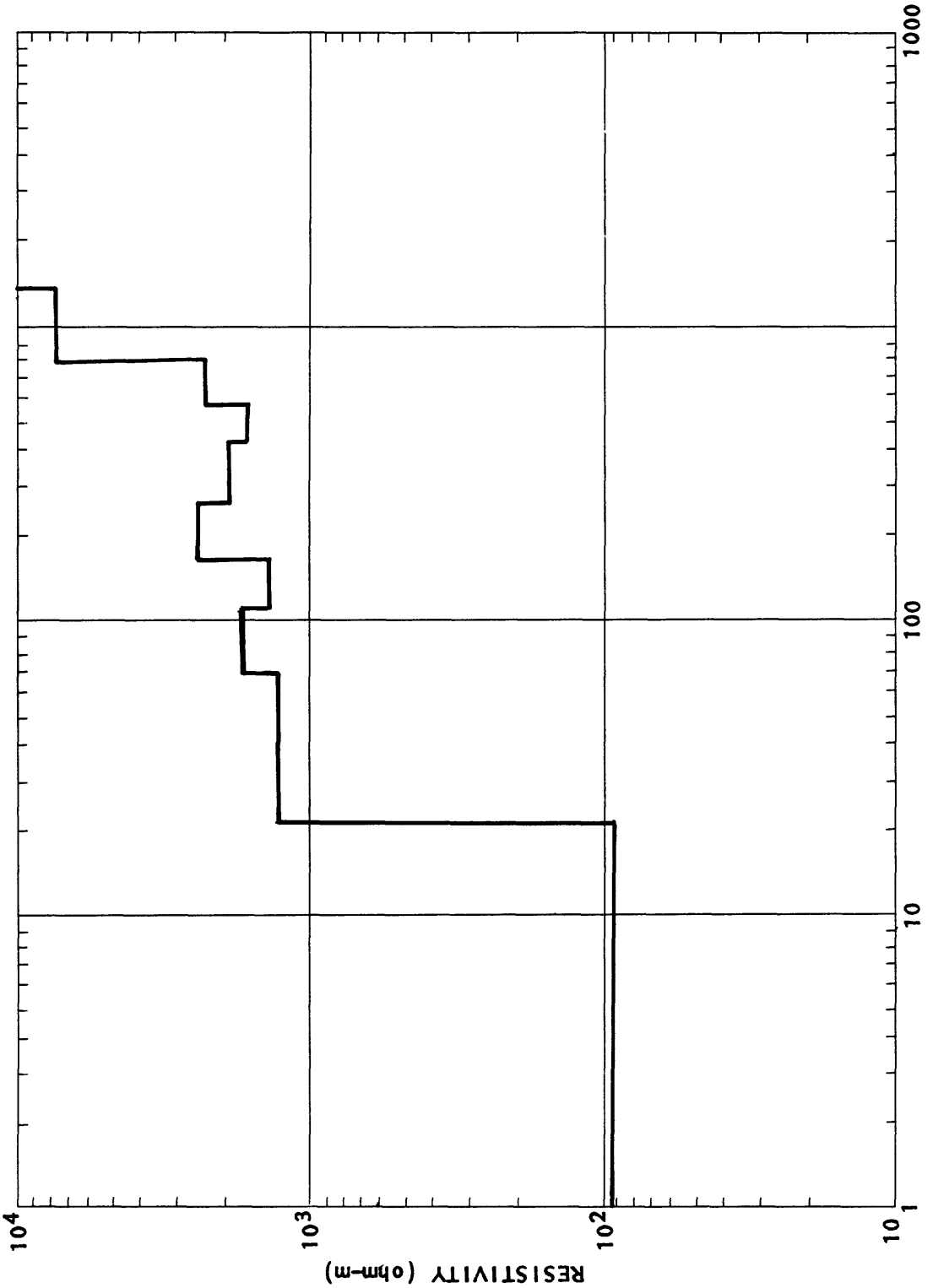

Silsilah AMT sounding F-11

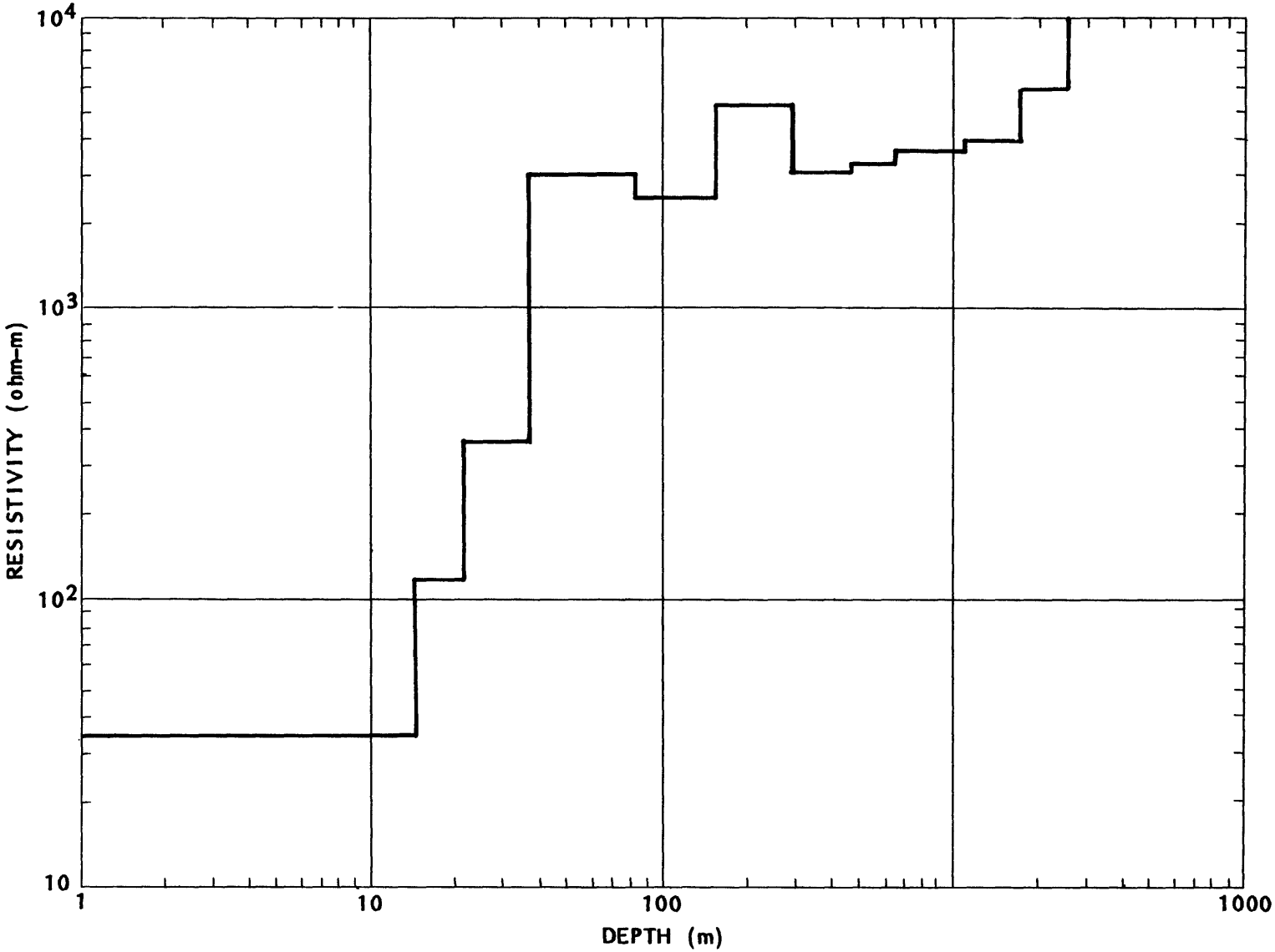

Silsilah AMT sounding F-12

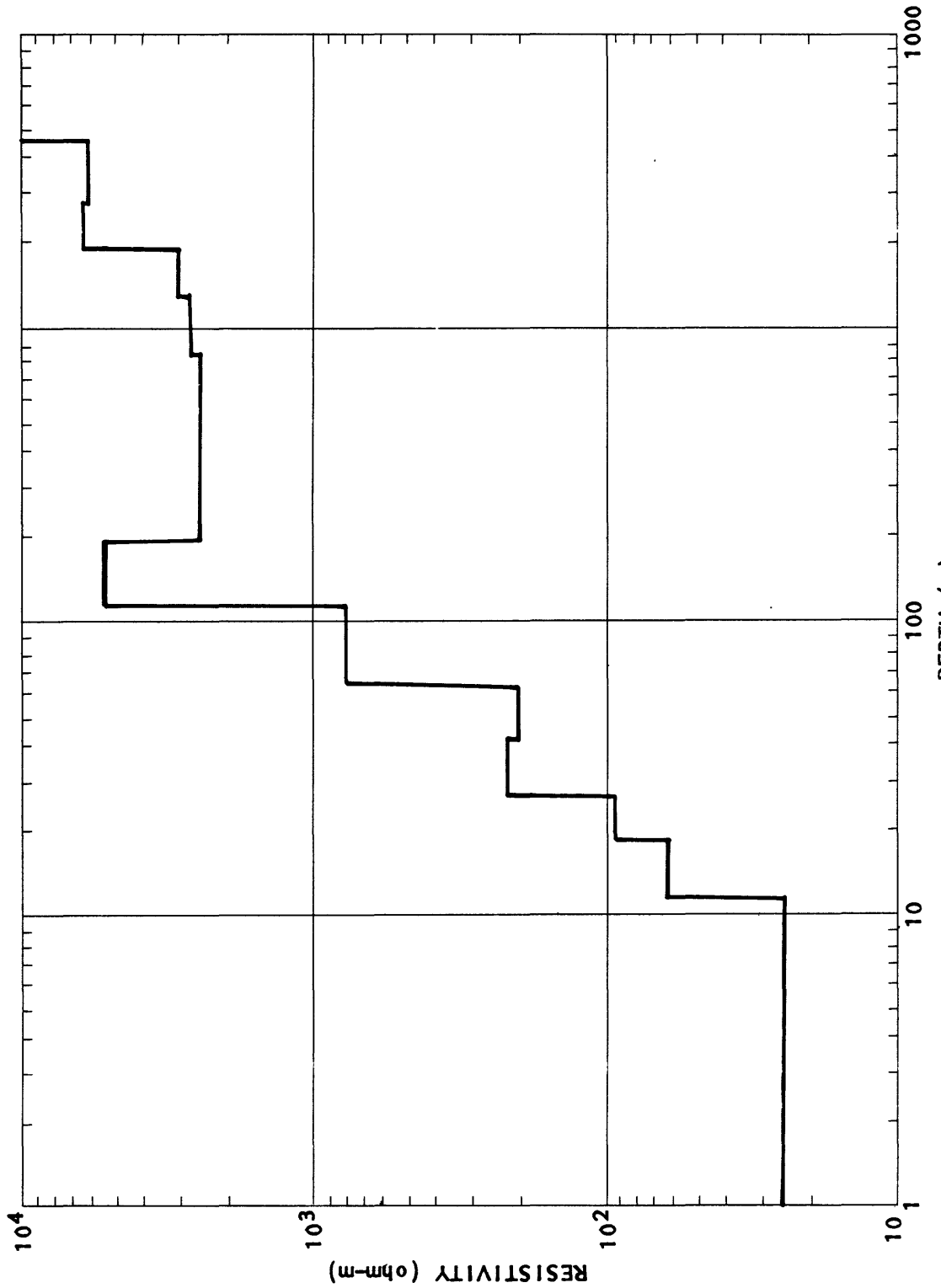

Silsilah AMT sounding F-13

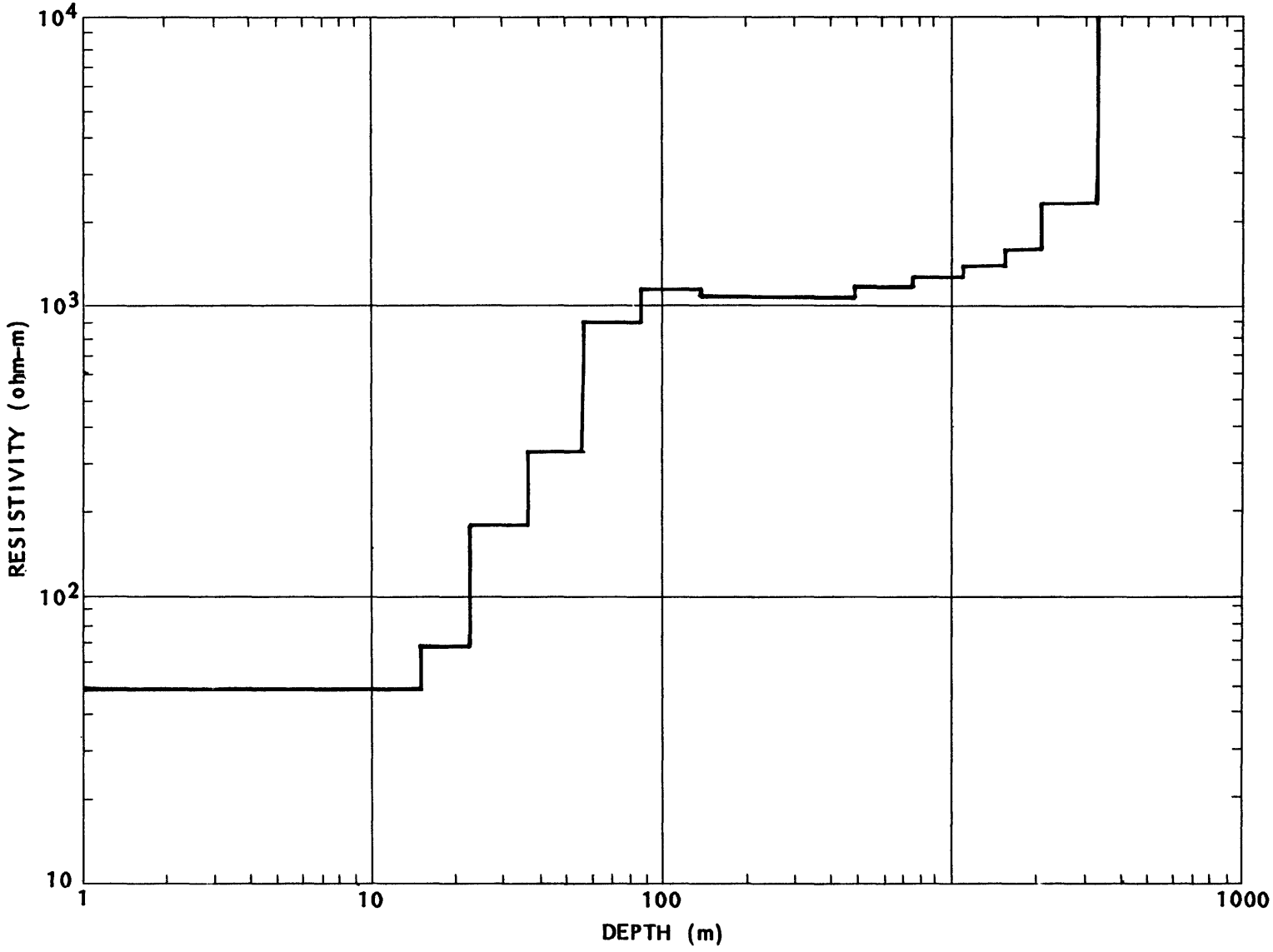

Silsilah AMT sounding F-14

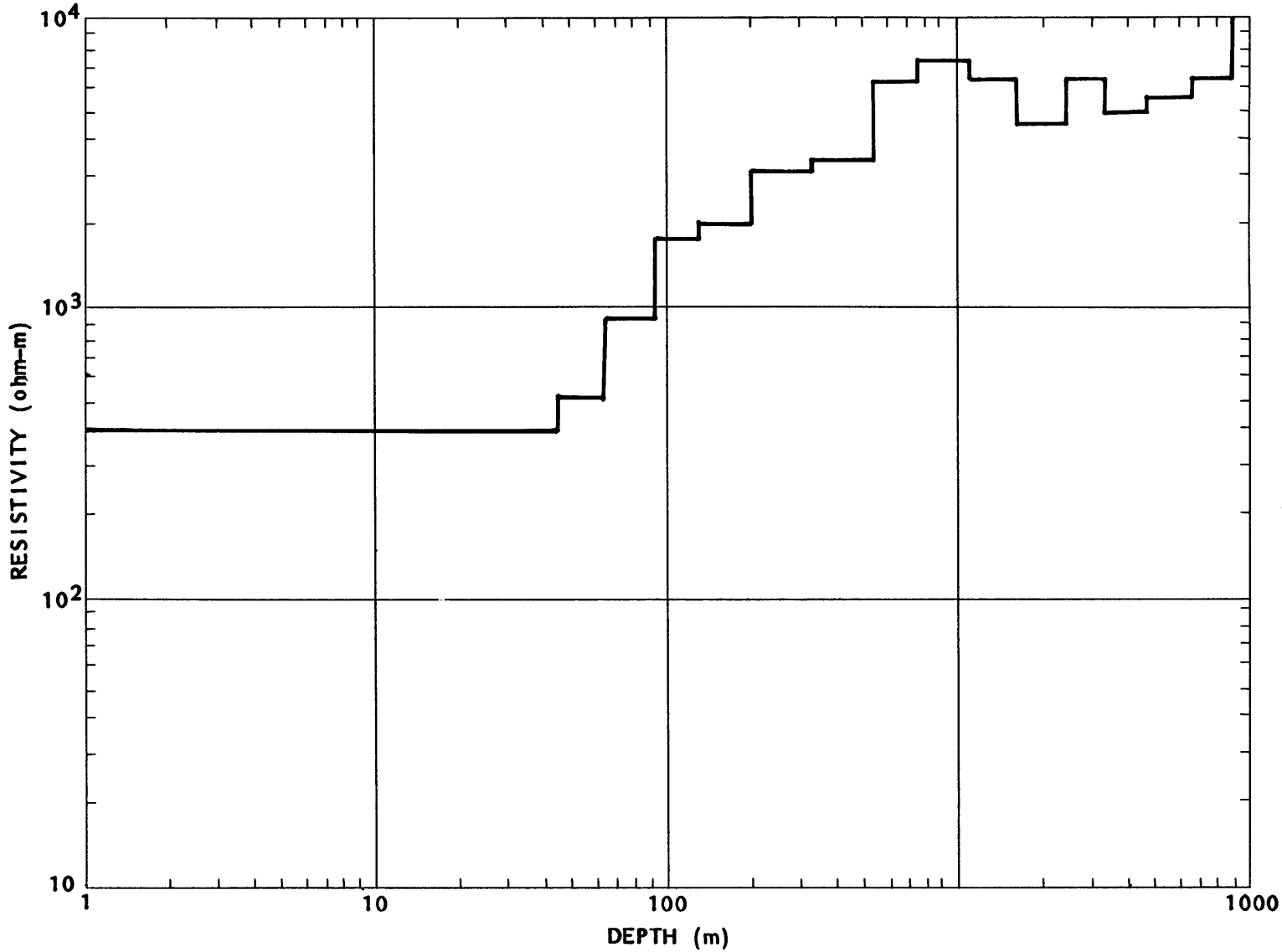

Silsilah AMT sounding F-15 interpreted geoelectric section